Marine and Petroleum Geology 69 (2016) 146–167

Contents lists available at ScienceDirect

Marine and Petroleum Geology

journal homepage: www.elsevier.com/locate/marpetgeo

Research paper

Composition and provenance of the Macigno Formation (Late Oligocene–Early Miocene) in the Trasimeno Lake area (northern Apennines)

Ugo Amendola [a, b], Francesco Perri [b], Salvatore Critelli [b, *], Paolo Monaco [a], Simonetta Cirilli [a], Tiziana Trecci [a], Roberto Rettori [a]

[a] Dipartimento di Fisica e Geologia, Università di Perugia, Piazza Università, 1, 06123 Perugia, Italy
[b] Dipartimento di Biologia, Ecologia e Scienze della Terra, Università della Calabria, via Ponte Bucci, 87036, Arcavacata di Rende (CS), Italy

ARTICLE INFO

Article history:
Received 30 July 2015
Received in revised form
20 October 2015
Accepted 24 October 2015
Available online 28 October 2015

Keywords:
Composition
Provenance
Gravity flow deposits
Northern Apennines
Palaeoweathering
Palaeoenvironment

ABSTRACT

Sandstone petrography and mudstone mineralogy and geochemistry of the Late Oligocene–Early Miocene terrigenous deposits of the Macigno Fm. of the Trasimeno Lake area (Central Italy) provide new information on provenance, paleoenvironment, palaeoclimate, and geodynamics during the early stages of the northern Apennines foreland basin setting. Sandstones are rich in trace fossils and are quartz-ofeldspatic with various crystalline phaneritic (mostly granitoids) and medium-low grade metamorphic rock fragments. Volcanic and sedimentary lithic fragments are rare.

The mudstone mineralogy contains a large amount of phyllosilicates, quartz, and feldspars and small amount of calcite, which increases in the mid-part of succession.

Palaeoweathering indices (Chemical Index of Alteration with and without CaO value; CIA and CIA' respectively) suggest a source area that experienced low to moderate weathering and low recycling processes (on average, CIA = 66.4 and CIA' = 69.7). Furthermore, very low and homogeneous values of Rb/K ratios (<0.006) suggest weak to moderate weathering conditions.

The sandstone and mudstone composition reflects a provenance derived from uplifted crystalline rocks. The different amount in feldspars, the variety of lithic fragments, the occurrence of mafic and carbonate input, coupled with evidence of multi-directional flows, suggest a provenance from different source areas. The geochemical proxies indicate a provenance from both felsic and mafic sources, predominantly for the Maestà section that shows Cr/V values ranging from 1.15 to 3.36 typical of source areas composed of both felsic and mafic rocks. The Western-Central Alps are inferred to be the main source area of the Macigno foreland system, but significant signals from the Mesomediterranean Microplate are also testified. These new data suggest that the Macigno Fm. was probably located in a peculiar area which received either distal fine turbidite flows from the northernmost Alpine area and residual sandy debris flows coming from the westernmost Alps.

1. Introduction

The thrust belt-foreland system of Northern Apennines was characterized by a continuous eastward migration of depocentres reflecting detachment of subducted lithosphere as result of African-European collision in the Late Eocene and subsequent rollback during the Late Oligocene to Recent time (Van der Meulen et al., 1998; Dinelli et al., 1999; Barsella et al., 2009). During the Oligocene–Miocene, foredeep depocentres were filled by thick debris of turbidite deposits in continuous and complex depositional units. The Macigno Fm. represents the first depositional unit of the Late Oligocene–Early Miocene foreland basin system of northern Apennines, linked to Alpine sectors through longitudinal feeding of the foreland basin (Ricci Lucchi, 1986, 1990). The Macigno Fm. is traditionally divided into a westernmost and oldest portion (late Chattian), cropping out along the Tuscan coast and named "Macigno Costiero" and an eastern and younger portion (late Chattian-Aquitanian) named "Macigno Appenninico" thrust

* Corresponding author.
E-mail address: ugoamendola@gmail.com (U. Amendola).

http://dx.doi.org/10.1016/j.marpetgeo.2015.10.019
0264-8172/

eastward on the Marnoso-arenacea Formation in the Casentino area (Boccaletti et al., 1990; Milighetti et al., 2009 among others). The Modino–Cervarola–Trasimeno units and associated facies (now included in eastern Macigno) and the overlying Marnoso-Arenacea Fm. represent the Mid-Late Miocene foreland basin system, whereas, the depositional framework and basin architecture of the foreland system are well developed (Ricci Lucchi, 1986, 1990; Centamore et al., 2002; Guerrera et al., 2012b). Differently to Ricci Lucchi (1986, 1990), Valloni et al. (1991), Pandeli et al. (1994) and recently Barsella et al. (2009) indicated only one terrigenous source area for the Macigno Fm., identified with the western-central Alps. Other authors recently claim that alpine source interfingered with an increasing contribution from the emerging Apennines from the Early Miocene onward, involving the upper portion of the Macigno Formation, especially the Modino–Cervarola unit (Gandolfi et al., 1983; Andreozzi and Di Giulio, 1994; Di Giulio, 1999). According to Cornamusini (2002) and Cornamusini et al. (2002), new sedimentological and petrographic data suggest that the Corsica-Sardinian Hercynian basement is the source area of the debris flow and turbidite sandstones of the "Macigno Costiero". Thus, the

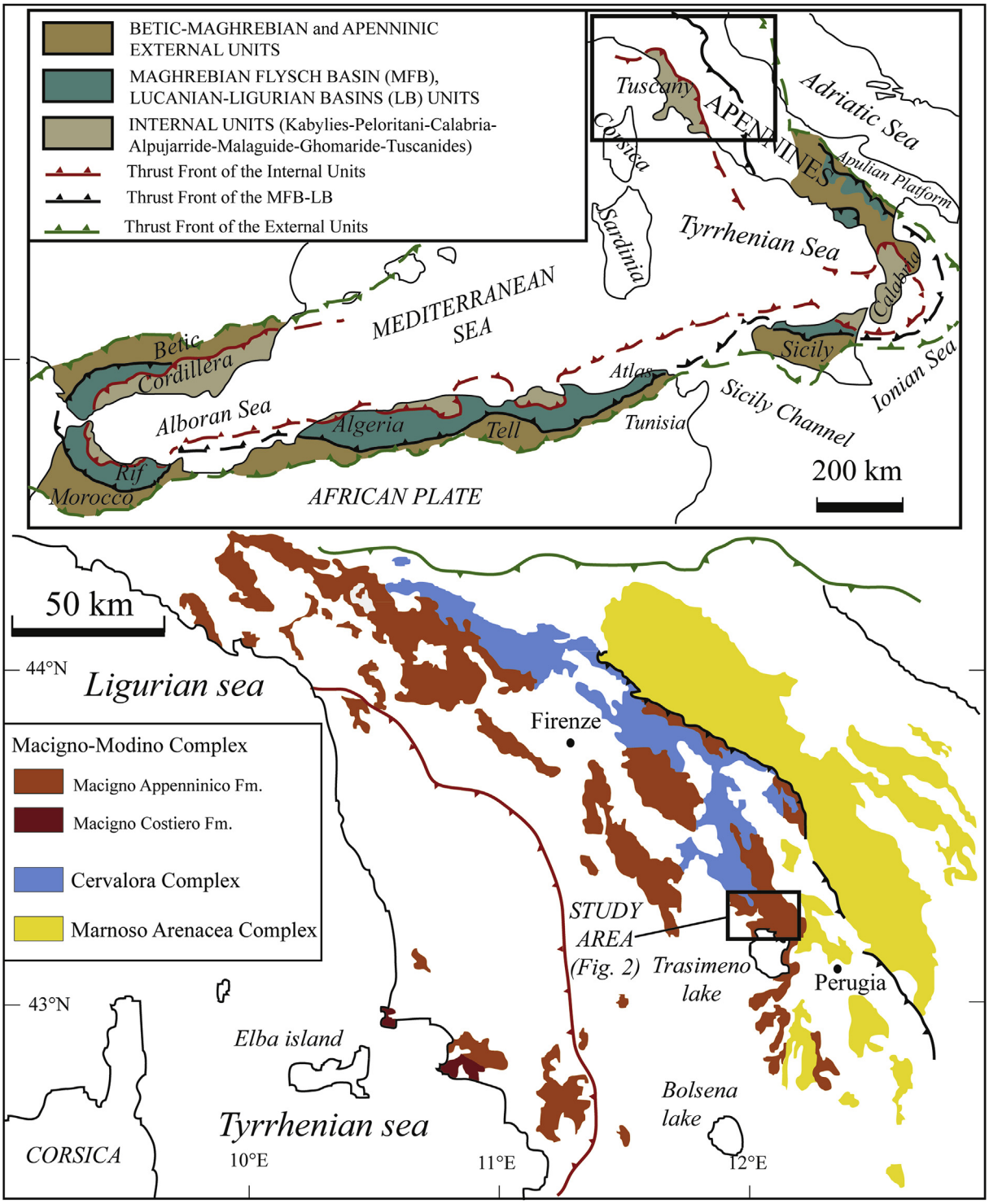

Fig. 1. Outcrop distribution of main Northern Apennines turbidite foredeep units, with indication of study area (modified after Dunkl et al., 2001).

hypothesis indicating a multi-source area for the Macigno Fm. can be strongly considered. In other models, a provenance from the Mesomediterranean microplate can also be suggested (e.g. Guerrera et al., 2012a, 2012b; Perrone et al., 2013; Guerrera and Manuel Martín-Martín, 2014, and bibliography therein).

Changes in sandstone composition of perisutural basins usually reflect complex provenance relationships from local to distal source areas, where long-distance transport is generally associated with Apenninic longitudinal orientation of flows. The local derivation of terrigenous, coarse grained and massive material is generally transverse from the west (e.g. Zuffa, 1987; Critelli et al., 1990; Critelli, 1993). This mixed provenance is typical of remnant ocean basin-fill (Critelli et al., 1990; Critelli, 1993) and foreland basin systems (Zuffa, 1987; Critelli, 1999; Critelli et al., 2007).

The aim of this work is to use a multi-disciplinary approach to provide useful information on the provenance of the Macigno Fm. sandstones for unraveling both local and distal terrigenous dispersal. For this purpose a detailed study of the Late Oligocene–Early Miocene sandstones and mudstones characterizing the Macigno Fm. of the Trasimeno Lake area, previously analyzed by sedimentological and ichnological point of view (Monaco and Trecci, 2014), has been done. The petrographical, mineralogical, and geochemical proxies are aimed to better understand the composition, provenance, and paleoclimatic signatures during the development of a foredeep basin system. Petrographic study of the coarse-grained fraction coupled with chemical and mineralogical analyses of the fine-grained fraction represents a thorough tool to investigate the processes that occurred from sediment generation on the exhumed uplands to the final deposition on foredeep basins. Detrital modes of sand reflect the cumulative effects of source rock composition, chemical weathering, hydraulic sorting, and abrasion (Suttner, 1974; Basu, 1985; Johnsson, 1993; Nesbitt et al., 1996).

The distribution of major and trace elements related to the mineralogical composition of fine-grained sediments is an important factor to reconstruct the source-area composition, the weathering and the diagenetic processes (e.g. Condie et al., 1992, 2001; Bauluz et al., 2000; Mongelli et al., 2006; Critelli et al., 2008; Zaghloul et al., 2010; Caracciolo et al., 2011; Perri, 2014; Perri and Ohta, 2014).

The X-ray diffraction (XRD) and X-ray fluorescence spectrometry (XRF) have been used to study and characterize the mineralogical and chemical variations of the mudstone samples, whereas the sand fraction has been studied by petrographic analysis. By combining the information deduced from these analyses, it is possible to outline possible variations on source areas and, thus, to explain and predict the sedimentary evolution and geological processes affecting the studied sediments.

Moreover the relationship developed between source area and sedimentary basin can be also defined.

2. Geological setting

The Northern Apennines are basically composed of two tectonic complexes: (1) the remnants of a Cretaceous–Paleogene accretionary wedge (Ligurian Complex), generated by the Africa–Europe convergence, thrust on top by (2) an Oligocene–Miocene terrigenous complex (Ricci Lucchi, 1986) that was accreted in a retreating subduction zone overriding the Adriatic continental margin (e.g., Castellarin, 1992). This second terrigenous complex is composed of different units: the Macigno and Modino turbiditic units of late Chattian to early Aquitanian age (25–23 Ma), the Monte Cervarola Fm. of late Aquitanian to early Langhian age (21–16 Ma), and the Marnoso-arenacea Fm. of Langhian to Tortonian age (14–9 Ma) (Guerrera et al., 2012b) (Fig. 1). The Late Oligocene–Early Miocene Macigno foredeep system was a basin 250–300 km in length, almost 50 km in width, and NW–SE oriented, starting from the modern Emilia (Northern Italy) to the Latium-Umbria border (Hill and Hayward, 1988; Boccaletti et al., 1990). The studied sections outcropping at the north of Trasimeno Lake (Fig. 2) belong to a N–S elongated Macigno Fm. basin deposited in the Tuscan Domain that

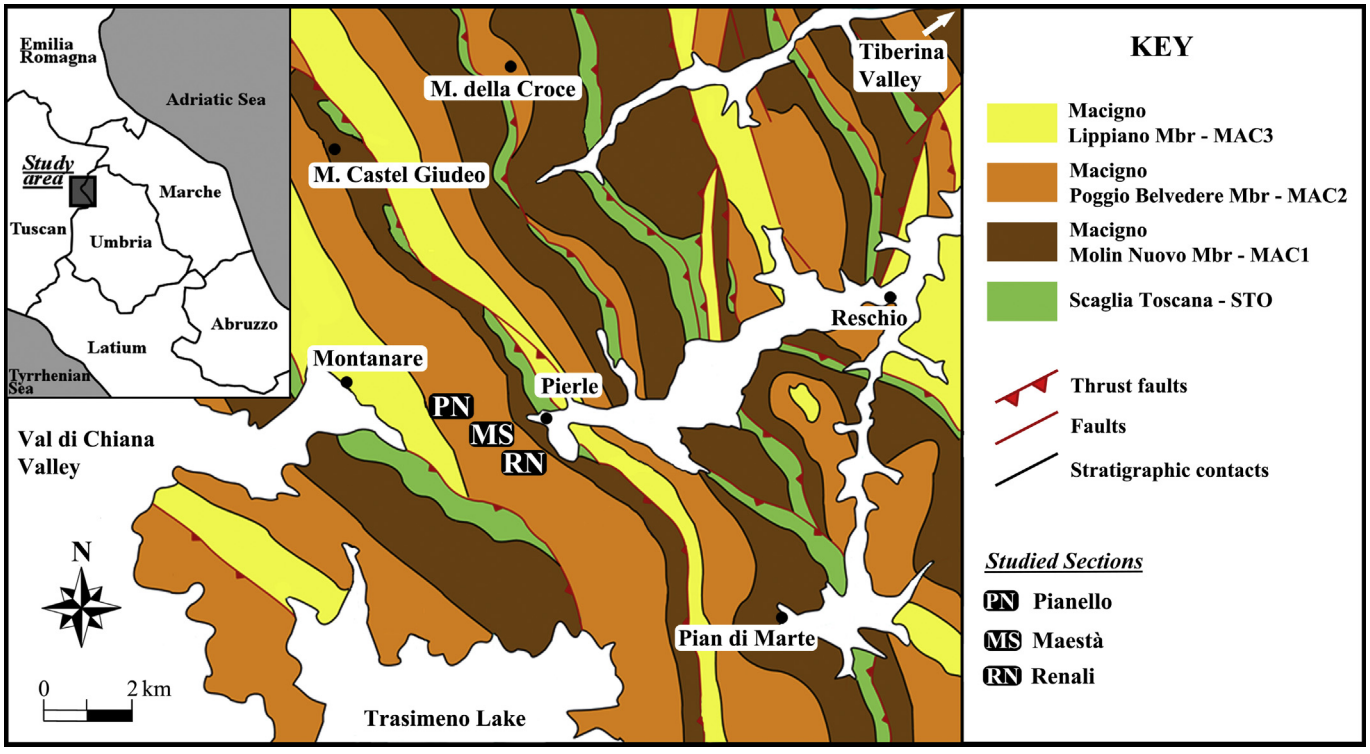

Fig. 2. Synthetic geological map of the Trasimeno Lake area showing outcrops of the Tuscan and Umbria successions and location of sections (after Monaco and Trecci, 2014).

were overthrust eastwards over the innermost sedimentary successions of the Umbria Domain (Canuti et al., 1965).

In the northern area of the Trasimeno Lake, the Macigno Fm. overlies the Scaglia Toscana Fm. (Cretaceous – Late Eocene) (Piccioni and Monaco, 1999; Plesi et al., 2002). The Scaglia Toscana Fm. (about 200 m thick) is made of limestones, marly limestones, variegated marls and dark pelitic beds with many coarse-to very fine-grained grained turbidites (Damiani et al., 1987; Ielpi and Cornamusini, 2013; Monaco et al., 2012). The Middle-Late Eocene portion is characterized by mud turbidites containing a typical deep-sea Nereites ichnofacies, with an ichnocoenosis at *Avetoichnus luisae, Chondrites intricatus, Cephalotes targionii, Cladichnus, Taenidium* and *Ophiomorpha rudis* (Monaco et al., 2012). These deposits show an increasing upwards contribution of clayey-marly and clayey lithotypes, respectively (Piccioni and Monaco, 1999; Monaco and Uchman, 1999; Monaco et al., 2012).

The Macigno Fm. is subdivided into three members: the Molin Nuovo Member (MAC1), the Poggio Belvedere Member (MAC2), studied in detail in this work, and the Lippiano Member (MAC3) (see detailed description in Trecci and Monaco, 2011). The Molin Nuovo Member in the lower portions of the Macigno Fm. (500–600 m of maximum thickness), consists of thick-bedded turbidites that pass upward to thinner strata. Facies assemblages indicate various deposits (in lithology and thickness), often arranged in thickening-upward sequences that can be related to depositional lobes of deep-sea fan (*sensu* Einsele, 1991). Thickening upward sequences are present even in the basal part of the Poggio Belvedere Member, while stationary sequences are common in the middle-upper portion of the Lippiano Member. Thick-bedded sandstones of outer lobes are interbedded with thinner arenaceous-pelitic and calcareous turbidites and lobe-fringe deposits of basin plain. The maximum thickness of the Poggio Belvedere Member is about 300 m, and its age has been attributed to the Chattian (MNP25b subzone, see Plesi et al., 2002 for the micropaleontological content). The lower units contain slurried beds (Ricci Lucchi and Valmori, 1980) and carbonate turbidites (Bruni and Pandeli, 1980; the Pietralavata Key-bed of Plesi et al., 2002; Brozzetti, 2007). Similar carbonate turbidites (the Polvano

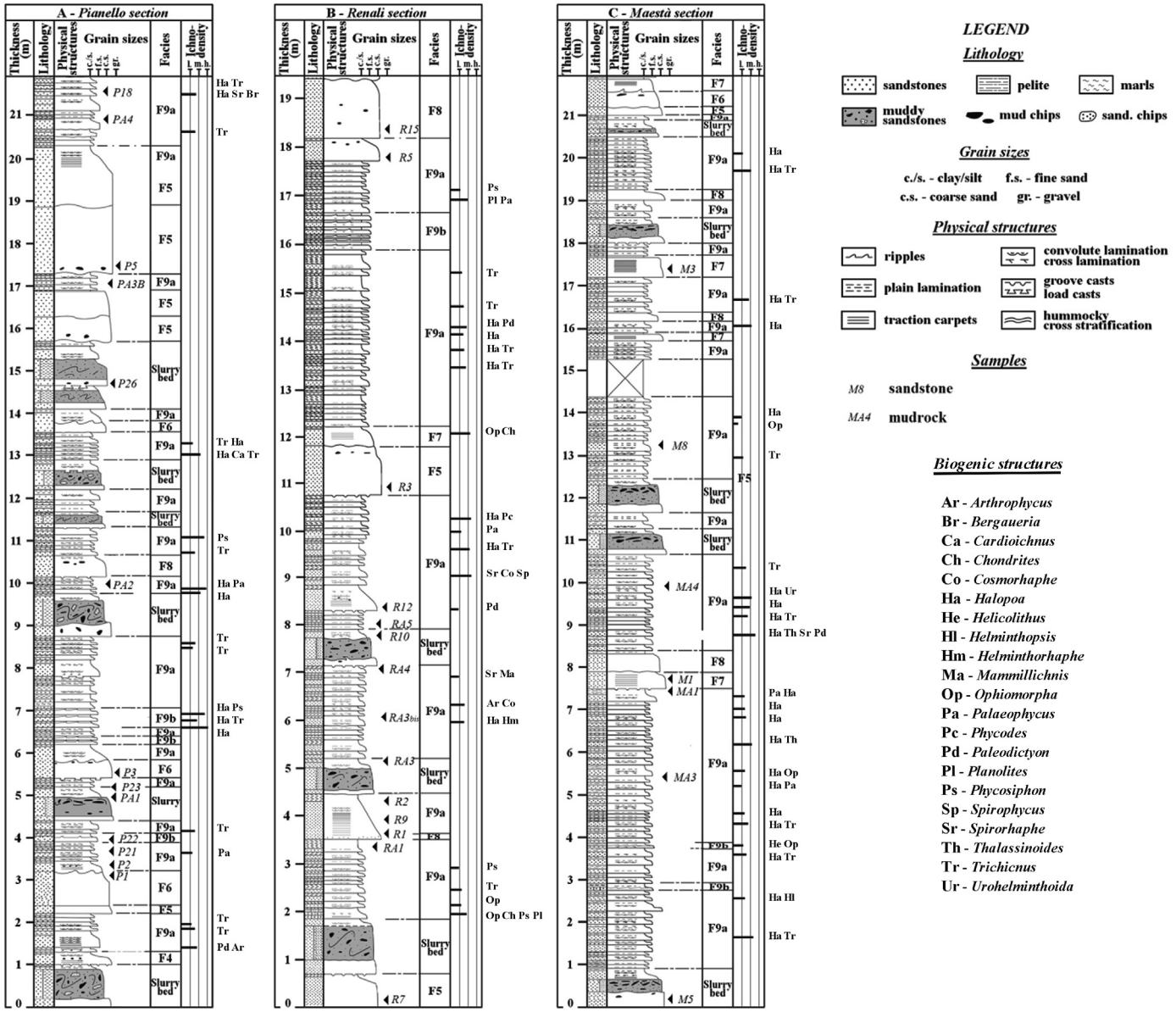

Fig. 3. Schematic synthetic stratigraphic columns of the Poggio Belvedere Member (MAC2), with the lithology and location of the studied samples. Pianello section (Lat. 43°15′08″, Long. 12°05′01″); Renali section (Lat. 43°14′41″, Long. 12°06′00″); Maestà section (Lat. 43°14′56″, Long. 12°05′41″).

Bed) are described by Aruta et al. (1998) for the Cortona area (Brozzetti, 2007). Nannofossil assemblages (Plesi et al., 2002) testify the Late Chattian-Early Aquitanian age (MNP25b-MNN1b) for the Poggio Belvedere Member. In the overlying Lippiano Member, the thinner facies, tabular beds (with flat basal surfaces and good lateral continuity, *sensu* Einsele, 1991) are dominant, typically of distal, basin plain environment. The calcareous beds are more frequent than in the Poggio Belvedere Member (Aruta, 1994; Aruta and Pandeli, 1995; Aruta et al., 1998). Biostratigraphic investigation (Plesi et al., 2002) suggests a Late Aquitanian age (MNP25b-MNN1b) for the Lippiano Member. In the overall Macigno Fm., multidirectional grooves and flute casts indicate mainly NW/SE oriented paleocurrents, with a SE preferential flow direction, and minor W oriented flows (e.g. slurried beds and slumps) (see in detail below).

3. Stratigraphy, facies and ichnocoenoses of the studied sections

Three stratigraphic sections belonging to Poggio Belvedere Mb. (MAC2) have been studied in the Trasimeno Lake area (Fig. 2), and were sampled for the purposes of the present study. The studied sections were sampled near Cortona along the SP35 road from Cortona (Tuscany) to Umbertide (Umbria) in three distinctive areas where are in stratigraphical continuity: the Pianello, Renali and Maestà Stratigraphic sections (Fig. 3).

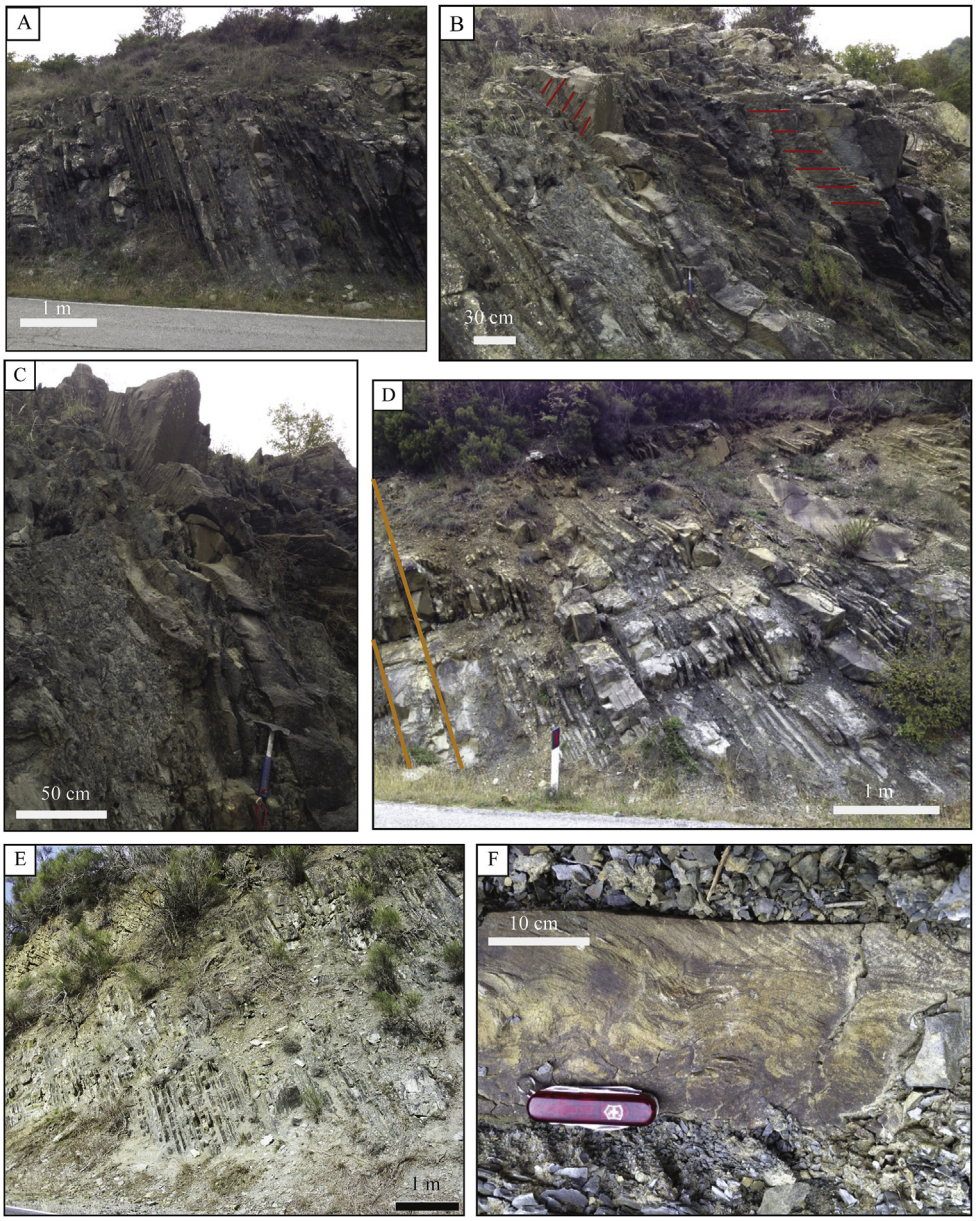

Fig. 4. Outcrops of the Poggio Belvedere Member in Trasimeno Lake area. (A) General view of the upper Pianello section deposits showing alternation between thin-bedded fine-grained turbidites (F9b facies of Mutti, 1992) and massive coarse-grained sandstones (F5–F7 facies of Mutti, 1992). (B) Detail of multidirectional lineations in sandy horizons in the uppermost portion of the Pianello Stratigraphic section (red lines indicate direction of palaeocurrents). (C) View of massive sandy horizons (F6 facies) including West-oriented flute casts in the upper Pianello Stratigraphic section. (D) View of mid-lower Renali section deposits, with presence of basal calcirudite and calcarenite levels (among yellow lines) interfingered within deep-water siliciclastic succession. (E) Alternating mudstones and fine-grained sandstones interfinged with thin massive coarse-grained sandy horizon at Maestà Stratigraphic section. (F) Detail of convolute laminations of a sandy level within fine-grained turbidite deposits (T_c of Bouma sequence) in the Maestà Stratigraphic section. (For interpretation of the references to colour in this figure legend, the reader is referred to the web version of this article.)

3.1. Pianello Stratigraphic section

The section (Fig. 4A–C) is more than 25 m in thickness and rests on the Early Oligocene Molin Nuovo Mb. (MAC1). The Pianello section is characterized by a diverse facies assemblage that includes massive to laminated thin-bedded coarse-grained turbidite sandstones (F5–F6–F7 facies of Mutti, 1992), up to 2–4 m in thickness, 0.5 m thick slurried beds (F1–F2 facies of Mutti, 1992) and an alternance of bioturbated hemipelagic mudstones and fine-grained turbidites (F8–F9a–b facies of Mutti, 1992).

The sandy horizons have been interpreted as transitional high-density turbidites (Mutti, 1992) or cohesive sandy debris flow deposits (Shanmugan, 2002). They partially include pebbles, mud lumps and several vegetal fragments and decrease in thickness going toward the mid-upper portion of the section in which the mudstones and mud turbidites begin to prevail. Fine-grained turbidites contain plane-parallel and convolute laminae and are associated to the T_{b-e} Bouma facies. These levels include a rich ichnocoenosis, typical of basin plain depositional area of the *Nereites* ichnofacies, mainly represented by hypichnial to epichnial and exichnial trace fossils (Monaco and Trecci, 2014). The abundant trace fossils are *Halopoa imbricate, Phycosiphon* sp., *Spirophycus bicornis.* The common trace fossils are *C. intricatus*, *Ophiomorpha rudis, Ophiomorpha annulata, Trichichnus* sp., *Spirorhaphe involuta,* whereas *Palaeophycus tubularis* is rare.

Slurried beds are easily recognizable for the inner subdivision of the beds in three intervals: a) coarse-grained basal sandstone interval, b) an intermediate swirly appearance (*sensu* Ricci Lucchi and Valmori, 1980) and, on the top, c) a fine-grained sandstone interval referred as F9a (Trecci and Monaco, 2011 and references therein). Slurried beds occur through the entire stratigraphical section and they are often intercalated with fine-grained turbidites. They come from a close slope area and probably are derived from co-genetic debrite-turbidite composite flows (Ricci Lucchi and Valmori, 1980; Talling et al., 2004; see types of Muzzi Magalhaes and Tinterri, 2010).

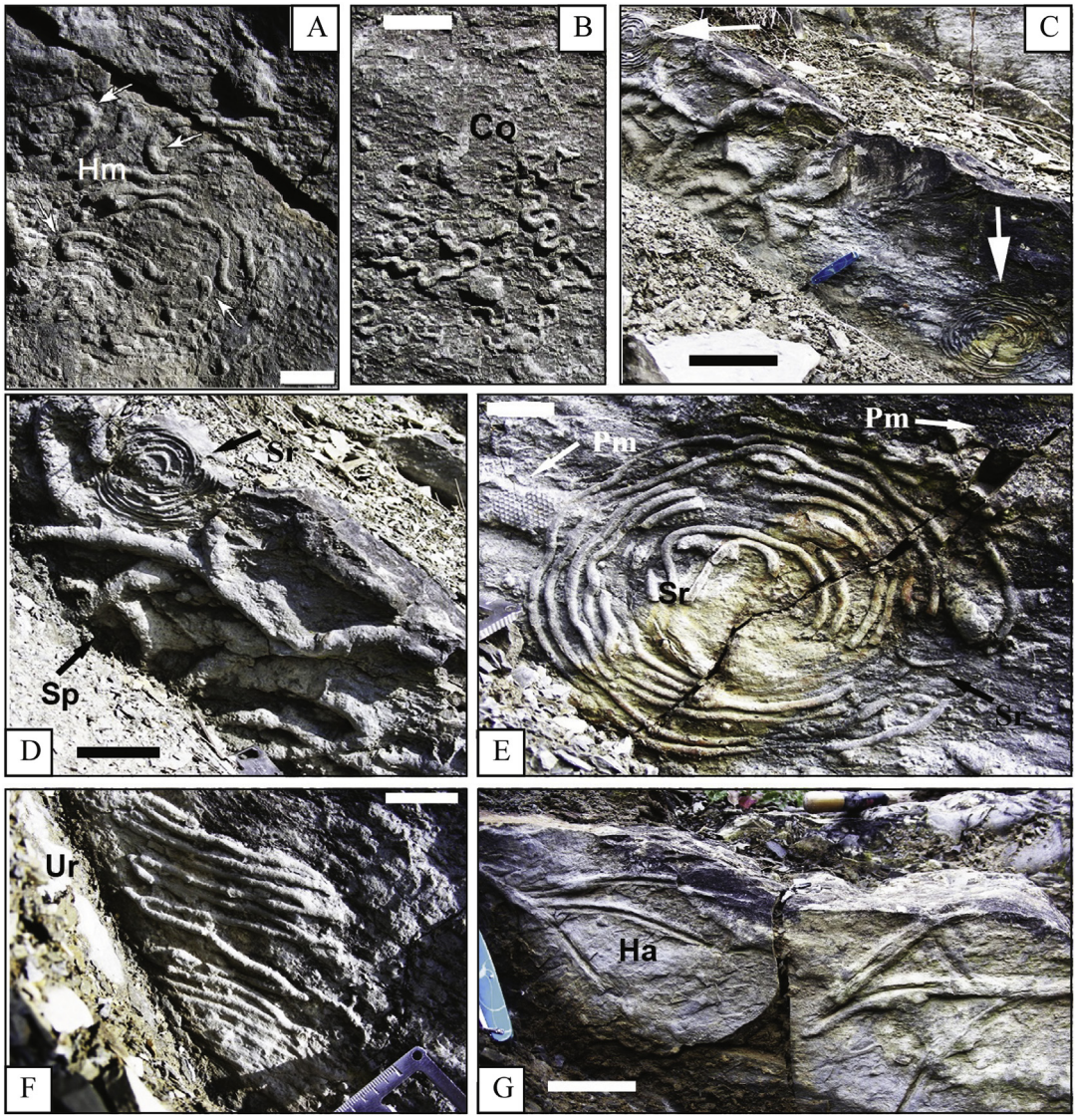

Fig. 5. Peculiar fossil traces in the studied sections. Renali Stratigraphic section (A–B): (A) The graphoglyptid *Helminthorhaphe* (Hm) at sole of turbidite with other undetermined curved specimens (arrows), bar = 3 cm; (B) The graphoglyptid *Cosmorhaphe isp.* at sole of turbidite, bar = 3 cm. Maestà Stratigraphic section (C–G): (C) a sole of thin turbidite with *Spirophycus* (centre) and *Spirorhaphe* (arrows), scale = 10 cm; (D) a detail of *Spirophycus* (Sp) and *Spirorhaphe* (Sr), bar = 10 cm; (E) a further detail on *Spirophycus bicornis* (Sp) and *Spirorhaphe* (Sr) with two *Paleodictyon minimum* specimens (Pm, arrows), bar = 5; (F) the hypichnial graphoglyptid *Urohelminthoida dertonensis* at sole of turbidite, bar = 5 cm; (G) Endichnial *Halopoa* (Ha, variation Fucusopsis) at sole of turbidite, bar = 10 cm.

Palaeocurrent data show predominant NW-oriented flows for fine-grained turbidites and some massive sandy horizons. However several groove casts, individuated in the uppermost facies of the coarse-grained sandstones and slurried divisions, clearly indicate W-oriented flows (Fig. 4B). Thus two types of groove casts have been recovered with an angle from 20 to 40°. The facies assemblage of Pianello Stratigraphic section reflects a transition from outer lobe, indicated by coarse-grained sandstone horizons, to fringe-basin plain facies, represented by fine-grained turbidites, and outlines a slight deepening of the depositional system.

3.2. Renali Stratigraphic section

The section (Fig. 4D) is more than 20 m thick and overlies deposits of the Pianello section. The section is characterized by an increase of rhythmical fine-grained turbidites (F9a–b facies). Laminated beds (T_b of Bouma facies) are thicker than the convolute laminae interval (T_c of Bouma facies) and they can reach 1 m in thickness.

Ichnocoenosis is quite similar to that analyzed in the previous section. Differences consist of larger amounts of *Ophiomorpha annulata, Halopoa*, *Phycosiphon*, *Planolites* and *Spirorhaphe*. Similarly to previous section *Spirophycus bicornis* is abundant whereas *Paleodictyon maximum and P. strozzii* are common. Also *Helmintorhaphe* sp. and *Cosmorhaphe lobata* occur (Fig. 5A–B) (Monaco and Trecci, 2014). Coarse-grained sandstone facies (F5–F6–F7 facies), up to 2 m thick, only appear in the basal and upper portion, and they are totally absent in the central part where fine-grained turbidites are dominant. Slurried beds, up to 1.5 m thick, show similar characteristics to those described for the previous section but they are less frequent. Moreover, in the basal portion of analyzed section, laminated to convoluted calciturbidite deposits, up 2–3 m thick, occur (Fig. 4D). They are well sorted, and have sharp basal contacts and tabular top surfaces and that include graded and laminated to convoluted Bouma T_{a-e} facies (Trincardi et al., 2005; Monaco et al., 2009; Trecci and Monaco, 2011).

Paleocurrent data show a NW-oriented flow for fine-grained turbidite facies. As seen in the previous section, multi-directional flows have been observed. In some thin laminated beds (F9b facies) flute casts clearly indicate W-oriented turbidite flows although groove casts individuated in calciturbidite levels show paleoflows towards the S and SW. The facies assemblage of Renali area thus reflects a basin plain environment, which locally received gravity flows coming from a very close slope area.

3.3. Maestà Stratigraphic section

The section (Fig. 4E–F) is more than 20 m thick and overlies deposits of Renali section and is overlain by Early Miocene Lippiano Mb. (MAC3). The section consists of mostly rhythmical, fine-grained turbidites (F9a-b facies) up to 5–6 m thick, which are interfingered by thin slurried beds, up 0.5 m thick and thin-bedded coarse-grained sandstones (F4–F7–F8 facies of Mutti, 1992), up 0.5–0.7 m thick. Laminated and convoluted facies (F9a-b facies of the same Author, Fig. 4F) are thinner than the Renali section, and the mudstone intervals are more abundant. The ichnocoenosis is dominated by an abundant endichnial/hypichnial *Halopoa* (both *Hydrostachys embricata* and *H.* var. *fucusopsis*), which occur in conspicuous amount in every thin beds, with *Spirorhaphe involuta* and *Urohelminthoida dertonensis*. *Chondrites*, *Paleophycus, Planolites, Ophiomorpha* and *Trichichnus* are rarer than in previous sections. Of particular significance is the occurrence of large *Spirophycus bicornis* with abundant *Spirorhaphe involuta, Paleodictyon minimum.* Also *P. strozzii* and *Urohelminthoida dertonensis* occur (Fig. 5C–F) (Monaco and Trecci, 2014).

Paleocurrent data only show NW-oriented flows. The Maestà section facies indicate a deeper basin plain environment, locally with turbidites and other residual gravity flows coming from a slope area that was probably farer than the depositional system depicted for Renali area.

4. Sampling and analytical methods

Sandstones and mudstones were sampled along the Poggio Belvedere Mb. (MAC2) in the Cortona area (Figs. 2 and 3). The sampling was concentrated in those parts of the succession, which are better exposed and preserved and thicker than in other analogue area of Trasimeno Lake. For the purpose of this study, we selected and analyzed only sandstone strata. Some strata show abundant carbonate particles (Renali area) characterized by carbonate clasts and fossils in both graded and laminated turbidite facies. These samples were only qualitatively described and not included in the recalculated analysis of the sandstones.

Nineteen medium-to coarse-grained sandstone samples were selected for thin-section preparation and modal analysis. Thin sections were etched with HF and stained by immersion in sodium cobaltonitrite solution to allow the identification of feldspars. More than 400 points were counted through the use of a petrographic microscope in each thin section according to the Gazzi-Dickinson method (Gazzi, 1966; Dickinson, 1970; Ingersoll et al., 1984; Zuffa, 1985). Recalculated grain parameters are defined according to Dickinson (1970), Ingersoll and Suczek (1979), Zuffa (1985), Critelli and Le Pera (1994, 1995), and Critelli and Ingersoll (1995).

Mudstone samples were crushed and milled in an agate mill to a very fine powder. The powder was placed in an ultrasonic bath at low power for a few minutes for disaggregation.

The mineralogy of the whole-rock powder was obtained by X-ray diffraction (XRD) using a Bruker D8 Advance diffractometer (CuKα radiation, graphite secondary monochromator, sample spinner; step size 0.02; speed 1 s for step) at the University of Calabria (Italy). Semiquantitative mineralogical analysis of the bulk rock was carried out on random powders measuring peak areas using the WINFIT computer program (Krumm, 1996). The strongest reflection of each mineral was considered, except for quartz for which the line at 4.26 Å was used instead of the peak at 3.34 Å because of its superimposition with 10 Å-minerals and I–S mixed layer series. The abundance of phyllosilicates was estimated measuring the 4.5 Å peak area. The percentage of phyllosilicates in the bulk rock was split on the diffraction profile of the random powder, according to the following peak areas: 10–15 Å (illite–smectite mixed layers), 10 Å (illite+micas), and 7 Å (kaolinite+chlorite) minerals (e.g. Cavalcante et al., 2007; Perri, 2008).

Whole-rock samples were prepared by milling to a fine powder in an agate mill. Elemental analyses for major and some trace elements (Nb, Zr, Y, Sr, Rb, Ba, Ni, Co, Cr, and V) were obtained by X-ray fluorescence spectrometry (XRF) using a Bruker S8 Tiger equipment at the University of Calabria (Italy), on pressed powder disks of whole-rock samples. These data were compared to international standard-rock analyses of the United States Geological Survey (e.g., Flanagan, 1976). The estimated precision and accuracy for trace element determinations are better than 5%, except for those elements having a concentration of 10 ppm or less (10–15%). Total loss on ignition (L.O.I.) was determined after heating the samples for 3 h at 900 °C.

5. Sandstone petrology and detrital modes

Samples include massive coarse-grained sandstones from the lobe-fringe facies (from F5 to F7 facies; Mutti, 1992), slurried divisions (F2 facies; related to residual dense flows), related to

residual dense flows, and graded-laminated sandstones from rhythmical fine turbidites (F8–F9a-b facies; related to low-density flows), related to low-density flows. The studied quartzofeldspathic sandstones are composed of moderately to poorly sorted, siliciclastic grains.

Raw point-count data of sandstones are in Table 1, whereas the recalculated modal point-count data are in Table 2.

a) Pianello Stratigraphic Section

Sandstones of the Pianello area range from massive sandstones of an outer lobe facies (P1, P23, P3, P5 samples) to fringe deposits of a basin plain (P2, P21, P22, P18 samples) with a single sample from a slurried division (P26 sample). The quartzofeldspathic sandstones have an average composition of $Qm_{48}F_{40}Lt_{12}$ (Fig. 6), and the Qm/F (Quartz monocrystalline/Feldspars) ratio is 1.33. These sandstones have variable sedimentary versus metasedimentary lithic fragments (average value: $Lm_{86}Lv_1Ls_{13}$; outer lobe facies: $Lm_{83}Lv_3Ls_{34}$; fringe-basin plain: $Lm_{88}Lv_0Ls_{12}$; slurried division: $Lm_{89}Lv_0Ls_{11}$; Fig. 6; Table 2). Feldspars (both plagioclase and K-feldspars) are the most abundant constituents in the lobe-fringe facies ($Qm_{39}F_{46}Lt_{15}$; Qm/F = 0.94). In particular feldspar content reaches the highest content in W-oriented grain flow deposits of the lobe facies (i.e. P5 = $Qm_{36}F_{49}Lt_{15}$; Qm/F = 0.73) of the mid-upper portions of the stratigraphic section. Plagioclase is dominant (average P/F = 0.66), and fresh grains are slightly more abundant than altered ones. Some plagioclase crystals display albite polysynthetic twinning (Fig. 7A). Quartz grains are also abundant, mainly as monocrystalline subrounded to angular and subspherical grains. Quartz grains are more prevalent in fringe-basin plain facies ($Qm_{55}F_{34}Lt_{11}$; Qm/F = 1.65) and slurried divisions ($Qm_{56}F_{39}Lt_5$;Qm/F = 1.44) than in the external lobe sandstones. Polycrystalline grains also occur in large amounts ($Qp_{73}Lvm_1Lsm_{26}$) and have similar tectonics-fabric versus plutonic-fabric. Dense minerals include garnet, epidote and zircon. Metasedimentary lithic grains are not abundant and they include phyllite, slate and fine-grained micaschist (Fig. 7B). Sedimentary rock fragments occur in discrete amounts in the outer lobe facies (i.e. P23 sample). A few volcanic lithic grains are also present (P23 sample) and they exhibit a felsic granular texture with plagioclase and minor quartz phenocrysts (Fig. 7C). Abundant phaneritic fragments of plutonic rocks, mostly plagioclase-rich granodiorite and tonalite, with minor granite (Fig. 7D), and coarse gneissic fragments also occur (average value; $Rg_{70}Rs_3Rm_{27}$; outer lobe facies: $Rg_{66}Rs_5Rm_{29}$; distal turbidite facies: $Rg_{73}Rs_2Rm_{25}$;

Table 1
Sandstone raw data. Categories used for sandstone samples point counts and assigned grains in recalculated plots are those of Zuffa (1985, 1987), Critelli and Le Pera (1994), and Critelli and Ingersoll (1995). R.f. = coarse grained rock fragments; NCE = noncarbonate extrabasinal grains; CI = carbonate intrabasinal grains.

		Poggio Belvedere member																		
		Pianello area									Renali area						Maestà area			
		P1	P23	P3	P5	P2	P21	P22	P18	P26	R7	R3	R12	R5	R10	R15	M1	M3	M8	M5
NCE	Quartz (single crystals)	85	39	89	54	65	90	112	85	121	87	124	89	103	116	118	105	183	142	133
	Polycrystalline quartz with tectonic fabric	6	9	17	19	14	13	12	12	5	6	10	12	7	11	7	8	6	4	4
	Polycrystalline quartz without tectonic fabric	11	8	19	10	11	12	9	16	4	4	10	5	6	13	5	3	0	4	2
	Quartz in metamorphic r.f.	3	0	4	7	1	4	2	3	0	1	3	1	7	2	1	1	0	0	2
	Quartz in plutonic r.f.	20	25	27	33	32	28	26	22	17	37	24	19	23	14	13	9	1	2	4
	Quartz in plutonic or gneissic r.f.	3	1	11	2	3	1	8	2	0	6	1	2	4	0	3	1	1	0	0
	Quartz in sandstone	0	1	0	0	0	0	0	0	0	0	0	0	0	0	0	0	0	0	0
	Calcite replacement on Quartz	7	7	15	4	20	12	17	59	22	15	28	31	17	20	27	17	6	25	1
	K-feldspar (single crystals)	33	29	17	8	32	27	11	17	30	24	10	11	22	14	21	21	3	19	17
	K-feldspar in metamorphic r.f.	0	1	2	1	0	1	7	1	0	0	0	0	0	0	0	0	0	0	1
	K-feldspar in plutonic r.f.	10	17	9	11	4	6	0	5	5	6	3	1	5	3	2	3	0	3	0
	K-feldspar in plutonic or gneissic r.f.	0	1	2	0	1	1	0	0	0	2	0	0	0	0	1	1	0	0	0
	K-feldspar in sandstone	0	0	0	0	0	0	0	0	0	0	1	0	0	0	0	0	0	0	0
	Calcite replacement on K-feldspar	2	2	3	9	3	1	4	4	10	1	0	0	0	1	3	1	0	5	0
	Plagioclase (single crystals)	59	53	36	35	34	39	32	27	51	35	43	58	35	35	45	55	37	34	65
	Plagioclase in metamorphic r.f.	1	4	0	5	0	0	1	0	0	0	0	1	1	1	0	0	0	0	0
	Plagioclase in plutonic r.f.	14	20	14	45	20	20	17	4	3	21	7	9	12	5	10	8	0	4	4
	Plagioclase in plutonic or gneissic r.f.	2	3	1	3	2	0	0	1	0	0	0	4	1	1	0	1	0	0	1
	Plagioclase in sandstone	0	1	0	0	0	0	0	0	0	0	0	0	0	0	0	0	0	0	0
	Calcite replacement on Plagioclase	16	12	5	19	20	9	9	12	12	5	3	9	1	16	7	11	0	5	0
	Micas and chlorite (single crystals)	21	16	12	25	27	24	34	35	28	34	19	23	41	29	37	50	67	49	69
	Micas and chlorite in plutonic r.f.	4	3	3	1	4	3	11	5	0	3	1	0	3	2	0	0	0	0	0
	Micas and chlorite in metamorphic r.f.	2	1	0	1	0	0	1	0	0	2	0	0	2	0	0	0	0	0	0
	Micas and chlorite in plutonic or gneissic r.f.	0	1	1	0	0	3	0	0	0	0	1	2	2	0	0	0	0	1	1
	Volcanic lithic with felsic granular texture	0	4	1	0	0	0	0	0	0	1	0	0	0	0	0	0	0	0	0
	Volcanic lithic with microlithic texture	0	0	0	0	0	0	0	0	0	2	0	0	2	1	0	0	0	0	0
	Other volcanic lithic	0	0	0	0	0	0	0	0	0	7	0	1	3	0	0	0	0	0	0
	Phyllite	5	3	6	6	4	2	0	3	0	3	3	1	2	1	0	0	0	1	0
	Fine grained schists	3	5	3	2	1	0	1	2	2	5	0	4	2	3	2	3	1	1	2
	Impure chert	1	2	2	2	0	2	0	0	1	0	2	2	0	1	0	5	2	1	0
	Sedimentary lithic	0	13	0	1	2	1	3	0	0	0	3	11	3	9	3	0	0	0	1
	Slate	3	4	1	1	1	1	1	1	1	2	4	2	1	1	0	0	0	0	1
	Chlorite/Muscovite schist	0	3	0	1	0	0	0	0	0	0	0	2	2	1	1	3	0	0	4
CE	Bioclasts	0	0	0	0	0	0	0	0	0	0	0	0	0	12	1	0	0	0	0
Mx	Siliciclastic matrix	46	30	56	4	41	54	33	1	40	24	28	31	49	79	3	28	2	12	30
	Epi matrix	1	0	2	3	2	1	3	1	0	0	0	0	0	1	4	1	3	3	0
	Pseudomatrix	0	0	0	6	17	4	1	3	0	1	1	2	2	0	1	4	6	3	7
Cm	Carbonate cement (pore-filling)	0	4	0	1	0	4	0	68	2	0	0	0	0	0	2	0	0	2	0
	Carbonate cement (patchy-calcite)	0	0	0	2	0	2	0	0	6	2	2	4	2	4	0	0	0	1	0
	Calcite replacement on undetermined grains	0	4	2	2	0	2	2	3	2	3	1	1	4	4	0	0	0	1	0
	Quartz overgrowth	0	1	0	0	0	0	0	0	0	0	0	0	0	0	0	0	0	0	0
TOT		358	327	360	323	361	367	357	392	362	339	332	338	364	400	317	339	318	322	349

Table 2
Recalculated modal point count data.

Section	Facies	Sample	%			%			%			%			%			%			%			%			Index			
			Qm	F	Lt	Qt	F	L	Qm	K	P	Qp	Lvm	Lsm	Lm	Lv	Ls	Rg	Rv	Rm	Rg	Rs	Rm	Lv/L	P/F	Q/F	F/L
Maestà area	slurried div.	M5	58	36	6	60	37	3	61	8	31	43	0	57	92	0	8	42	0	58	40	4	56	0	0.79	1.59	6.29
	basin plain	M8	68	28	4	71	28	1	70	12	18	82	0	18	86	0	14	63	0	37	59	6	35	0	0.61	2.41	6.36
	outer lobe	M3	79	17	4	83	16	1	83	1	16	89	0	11	78	0	22	22	0	78	18	18	64	0	0.92	4.77	4.44
	outer lobe	M1	52	39	9	58	39	3	57	11	32	73	0	27	74	0	26	61	0	39	53	12	35	0	0.74	1.32	4.59
		outer lobe	66	28	6	71	27	2	70	6	24	81	0	19	76	0	24	42	0	58	36	15	49	0	0.83	3.045	4.52
		X	***64***	***30***	***6***	***68***	***30***	***2***	***68***	***8***	***24***	***72***	***0***	***28***	***82***	***0***	***17.5***	***47***	***0***	***53***	***42.5***	***10***	***47.5***	***0***	***0.76***	***2.52***	***5.42***
		s.d.	***12***	***9.83***	***2.36***	***12***	***10***	***1.15***	***12***	***5***	***8.42***	***20***	***0***	***20***	***8.06***	***0***	***8.06***	***19***	***0***	***19***	***18***	***6.32***	***15***	***0***	***0.13***	***1.57***	***1.05***
Renali area	slurried div.	R15	65	27	8	65	33	2	64	11	25	67	0	33	71	0	29	72	0	28	67	7	26	0	0.7	1.82	4.94
	slurried div.	R10	54	27	19	66	28	6	67	8	25	61	2	37	42	3	55	54	2	44	46	18	36	0.04	0.76	2	1.81
		slur.div.	59.5	27	13	65	31	4	66	9	25	64	1	35	56.5	1	42	63	1	36	57	12	31	0.02	0.73	1.91	3.375
	basin plain	R5	59	30	11	64	30	6	67	12	21	46	18	36	63	23	14	63	6	31	64	4	32	0.23	0.65	2	2.75
	basin plain	R12	52	34	14	58	34	8	60	5	35	47	3	50	60	3	37	66	1	33	56	16	28	0.03	0.87	1.53	2.32
		basin	56	32	12	61	32	7	64	8	28	46	11	43	61	13	26	64	4	32	60	10	30	0.13	0.76	1.765	2.535
	outer lobe	R3	67	25	8	72	24	4	73	6	21	69	0	31	77	0	23	65	0	35	59	9	32	0	0.79	2.69	2.09
	outer lobe	R7	54	35	11	58	35	7	61	14	25	33	34	33	62	38	0	72	10	18	80	0	20	0.38	0.65	1.55	3.13
		outer lobe	61	30	9	65	30	5	67	10	23	51	17	32	69	19	11.5	68	5	27	70	4	26	0.19	0.72	2.12	2.61
		X	***58.5***	***30***	***12***	***64***	***31***	***5***	***65***	***10***	***25***	***54***	***9***	***37***	***62.5***	***11***	***26***	***65***	***3***	***31.5***	***62***	***9***	***29***	***0.11***	***0.74***	***1.93***	***2.84***
		s.d.	***6.28***	***4.08***	***4.17***	***5.31***	***4.18***	***2.17***	***4.76***	***3.56***	***5.13***	***14***	***14***	***6.89***	***12***	***16***	***19***	***6.68***	***4***	***8.55***	***11***	***6.93***	***5.62***	***0.16***	***0.09***	***0.43***	***1.13***
Pianello area	slurried div.	P26	56	39	5	60	39	1	59	17	24	77	0	23	89	0	11	76	0	24	73	3	24	0	0.59	1.44	8.54
	fringe-basin	P18	62	26	12	72	26	2	71	11	18	82	0	18	100	0	0	64	0	36	64	0	36	0	0.62	2.4	2.09
	fringe-basin	P22	62	30	8	68	30	2	67	9	24	81	0	19	78	0	22	71	0	29	69	3	28	0	0.73	2.03	3.11
	fringe-basin	P21	50	39	11	60	39	1	57	15	28	87	0	13	84	0	16	75	0	25	72	3	25	0	0.65	1.29	3.35
	fringe-basin	P2	45	43	12	54	43	3	51	17	32	76	0	24	91	0	9	90	0	10	88	3	9	0	0.65	1.04	3.51
		fringe-basin	55	34	10.75	63	35	2	62	13	25	81	0	19	88.25	0	11.75	75	0	25	73	2	25	0	0.6625	1.69	3.015
	outer lobe	P5	36	49	15	47	49	4	43	12	45	74	0	26	91	0	9	69	0	31	67	2	31	0	0.78	0.73	3.48
	outer lobe	P3	52	31	17	65	31	4	62	14	24	78	2	20	90	3	7	66	1	33	66	2	32	0.09	0.63	1.64	1.82
	outer lobe	P23	27	54	19	35	54	11	34	23	43	37	8	55	56	9	35	68	4	28	61	14	25	0.09	0.65	0.51	2.8
	outer lobe	P1	42	48	10	48	48	4	46	18	36	62	0	38	94	0	6	70	0	30	69	1	30	0	0.67	0.86	4.72
		outer lobe	39	46	15.25	49	45	6	46	17	37	63	2	35	82.75	3	34	68	1	31	66	5	29	0.045	0.6825	0.935	3.205
		X	***48***	***40***	***12***	***57***	***40***	***3***	***54***	***15***	***30***	***73***	***1***	***26***	***86***	***1***	***13***	***72***	***1***	***27***	***70***	***3***	***27***	***0.02***	***0.66***	***1.327***	***3.713***
		s.d.	***12***	***9.55***	***4.37***	***12***	***9.55***	***3***	***12***	***4.23***	***9.28***	***15***	***2.67***	***13***	***13***	***3***	***10***	***7.74***	***1.33***	***7.48***	***7.75***	***4.1***	***7.48***	***0.04***	***0.058***	***0.621***	***2***

Note: X = mean, s.d = standard deviation. Qm = monocrystalline quartz, Qp = polycrystalline quartz, F = feldspars (K+P), K = K-feldspar, P = plagioclase; Lt = lithic grains; Lm = metamorphic, Lv = volcanic, and Ls = sedimentary lithic grains; Lvm = volcanic and metavolcanic, Lsm = sedimentary and metasedimentary lithic grains; Rg = phaneritic plutonic rock fragments; Rm = coarse and fine grained metamorphic rock fragments; Rv = coarse and fine grained volcanic rock fragments; Rs = coarse and fine grained sedimentary rock fragments.

slurried division: $Rg_{73}Rs_3Rm_{24}$). In the outer lobe facies samples, several high-medium grade metamorphic (Fig. 7E) and some sedimentary fragments occur.

Lithic fragments, especially felsic volcanic fragments, in sandstone modes of the Pianello area are less abundant than those from the Macigno Fm. (Fig. 8; Table 3). In detail, sandstones of outer lobe facies are more feldspar-rich than sandstones of both "Macigno Appenninico" of Northern Tuscany (Di Giulio, 1999: $Qm_{59}F_{29}Lt_{17}$; Bruni et al., 2007: average value, $Qm_{50}F_{34}Lt_{16}$) and the "Macigno Costiero" of Southern Tuscany (Cornamusini, 2002: $Qm_{57}F_{19}Lt_{24}$). Also Poggio Belvedere sandstones of this study are more feldspar-rich than sandstones analyzed by Barsella et al., 2009 ($Qm_{36-61}F_{14-24}Lt_{10-25}$; Fig. 8). However, Plesi et al (2002) report a similar feldspar-rich trend in the lower sandstones of Poggio Belvedere Mb. collected in the High Tiber valley (Umbria). Likely, Bruni et al. (2007) point out a slight feldspar enrichment at the transition of the Lower-Upper Macigno Fm. in Abetone area (NW Tuscany) (max F = 35.6%, $Qm_{44}F_{44}Lt_{12}$; see GO 24 sample in Fig. 8). Differently, sandstones of basin plain facies have a composition that can be comparable with the average value indicated for the Macigno Fm. (Valloni et al., 1991; Di Giulio, 1999; Bruni et al., 2007; Barsella et al., 2009) (Table 3).

b) Renali Stratigraphic Section

Sandstones collected along the Renali stratigraphic section are in outer lobe-fringe facies (R7 and R3 samples), basin plain facies (R12 and R5 samples) and slurried divisions (R10 and R15 samples). Other samples were collected in the calcareous turbidite facies (R1, R2 and R9 samples) but they were not counted but only qualitatively described. The sandstone composition is quartzofeldspathic (average value: $Qm_{59}F_{30}Lt_{12}$; outer lobe-fringe facies: $Qm_{61}F_{30}Lt_9$; basin plain facies: $Qm_{56}F_{32}Lt_{12}$; slurried division: $Qm_{60}F_{27}Lt_{13}$). The average Qm/F ratio is 1.93.

These sandstones have similar amounts of sedimentary versus metasedimentary lithic fragments (average value: $Lm_{63}Lv_{11}Ls_{26}$; outer lobe facies: $Lm_{69}Lv_{19}Ls_{12}$; basin plain facies: $Lm_{61}Lv_{13}Ls_{26}$; slurried division: $Lm_{57}Lv_1Ls_{42}$; Fig. 6). Quartz grains are the most abundant constituents in all the sampled facies and their amount remain almost homogeneous with a slight peak in the outer lobe facies. Quartz grains show the same textural characteristics seen in the previous section, with a sharp prevalence of monocrystalline grains on polycrystalline grains, more marked than in the previous section ($Qp_{54}Lvm_9Lsm_{37}$) (Fig. 7F). Feldspars (both plagioclase and K-feldspars) are also abundant and maintain a constant ratio with the quartz grains. Many feldspar grains are altered; they are

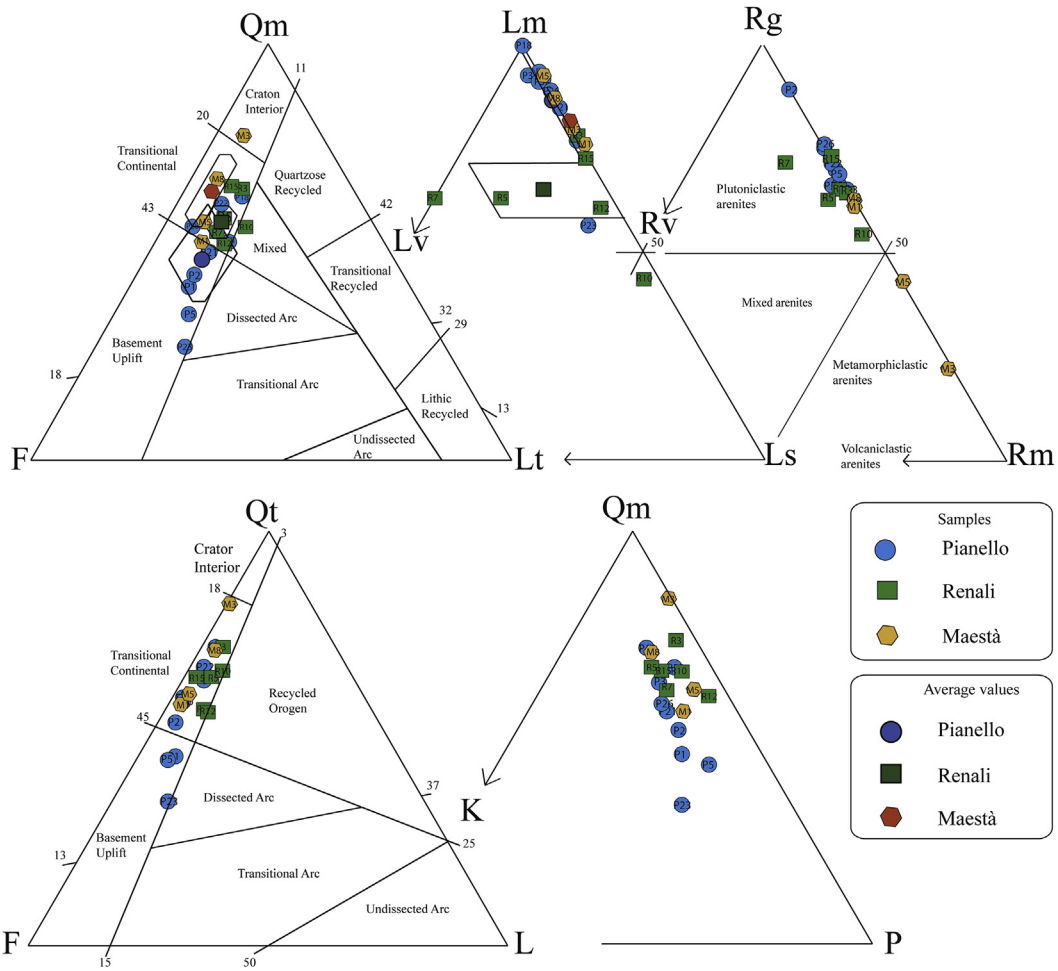

Fig. 6. Qm–F–Lt, Lm–Lv–Ls, Rg–Rs–Rm Qt–F–L and Qm–K–P triangular plots (from Dickinson, 1970; Ingersoll and Suczek, 1979; Critelli and Le Pera, 1994; Folk, 1968; Graham et al., 1976) for Poggio Belvedere sandstones of the Macigno Fm. Qm (monocrystalline quartz), F (feldspars) and Lt (total lithic fragments); Lm (metamorphic), Lv (volcanic) and Ls (sedimentary) lithic fragments; Rg (plutonic rock fragments), Rv (volcanic rock fragments) and Rm (metamorphic rock fragments); Qt (quartz grains), F (feldspars) and L (aphanitic lithic fragments); Qm (monocrystalline quartz), K (K-feldspar) and P (plagioclase).

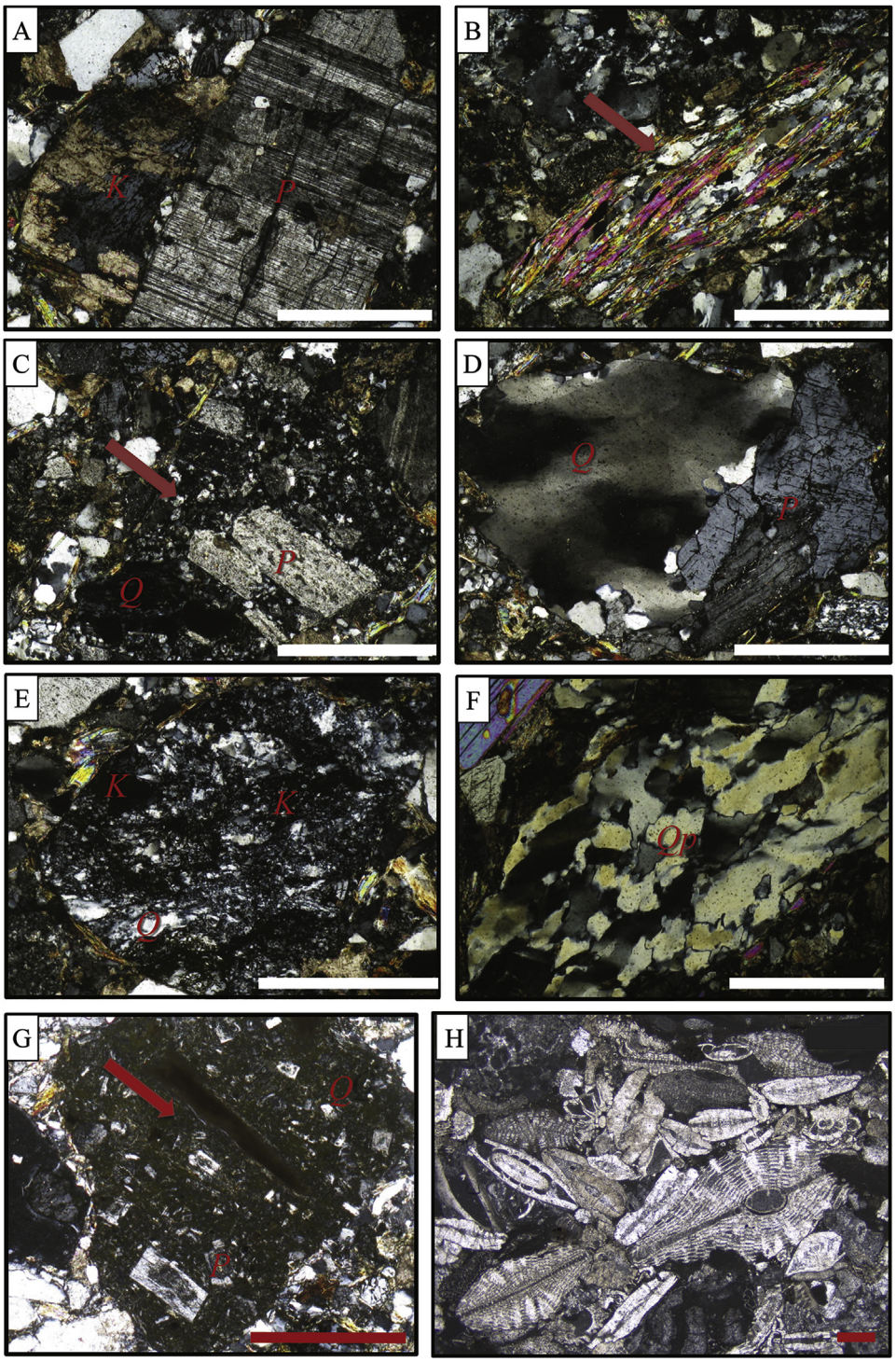

Fig. 7. Peculiar granular components in sandstones (crossed nicols view), bar = 500 μm. (A) Plagioclase displaying typical albite polysynthetic twinning (*P*) and K-feldspar grains (*K*) locally replaced by calcite cement. (B) Fine-grained schist (*red arrow*) with internal muscovite and quartz grains. (C) Volcanic rock fragment with felsic granular fabric (*red arrow*) including internal plagioclase (*P*) and quartz (*Q*) phenocrysts. (D) Plutonic rock fragment with quartz (*Q*) and plagioclase crystals (*P*). (E) Metamorphic rock fragment with isoriented strips of quartz (*Q*) and K-feldspar (*K*). (F) Polycristalline quartz grain with tectonic fabric (*Qp*). (G) Volcanic rock fragment with microlithic fabric (*red arrow*) containing phenocrysts of plagioclase (*P*) and quartz (Q) in a fine-grained groundmass rich in K. (H) Packstone with macroforaminifers (lepidocyclinids and nummulitids). (For interpretation of the references to colour in this figure legend, the reader is referred to the web version of this article.)

sericitized and partially clay altered. The plagioclase versus total feldspars ratio is higher than that of the previous section (P/F = 0.74). Metasedimentary lithic grains are not so abundant and they include phyllite, slate and fine-grained micaschist, including also few chloriteschist fragments. Siltstone and chert fragments are also present. Volcanic lithic fragments are more abundant than in the other sections (with a prevalence in R7 sample) and they occur in both outer lobe and distal turbidites facies (Fig. 7G). Abundant phaneritic fragments of plutonic rocks, mostly plagioclase-rich granodiorite and tonalite, with minor granite also occur (average

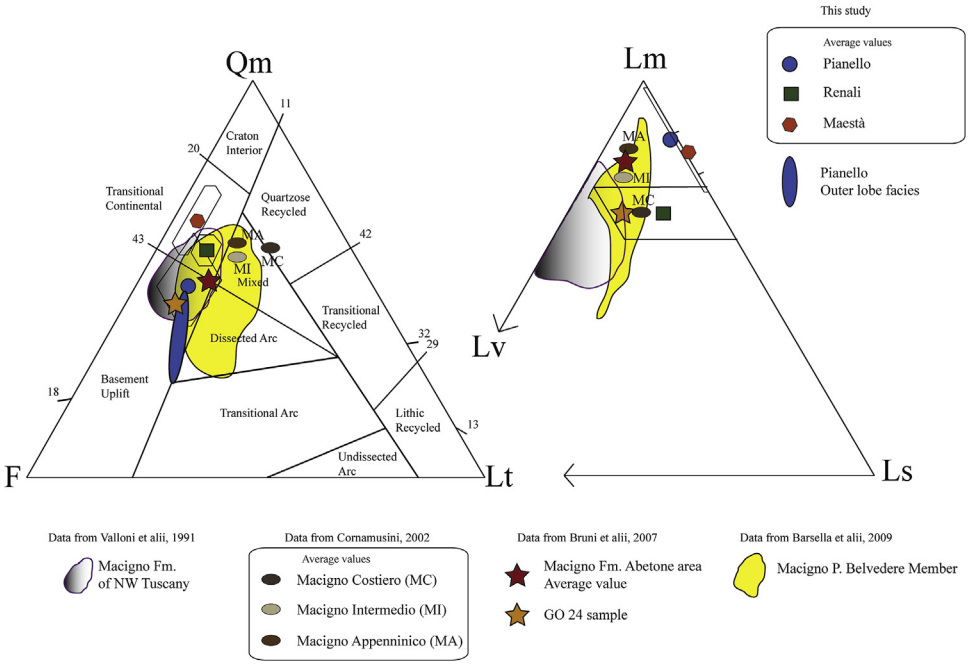

Fig. 8. Comparisons of studied data with previous works using Qm–F–Lt and Lm–Lv–Ls diagram plots (from Dickinson, 1970; Ingersoll and Suczek, 1979). Qm (monocrystalline quartz), F (feldspars) and Lt (total lithic fragments); Lm (metamorphic), Lv (volcanic) and Ls (sedimentary) lithic fragments.

Table 3
Average petrological parameters and ratios of Poggio Belvedere sandstones compared with Macigno sandstones and Calabrian arc sands (after Ibbeken and Schleyer, 1991; Perri et al., 2012b); standard deviation in brackets.

Clastic system	Petrological parameters and ratios										
	Qm	F	Lt	Lm	Lv	Ls	Lv%	Iv%	Q/F	F/L	P/F
Poggio Belvedere sandstones (this study)											
Maestà area	64 (12)	30 (10)	6 (2)	82 (8)	0	18 (8)	0	0	2.52	5.42	0.76
Renali area	59 (6)	30 (4)	12 (4)	63 (12)	11 (16)	26 (19)	14	11.25	1.93	2.84	0.74
Pianello area	48 (12)	40 (10)	12 (4)	86 (13)	1 (3)	13 (10)	4-2,5	2	1.33	3.71	0.66
Macigno sandstones – northern Tuscany (Di Giulio, 1999)											
Upper Macigno	54 (4)	29 (4)	17 (3)	84 (5)	11 (3)	5 (2)	…	…	1.9	1.8	…
Lower Macigno	55 (5)	26 (3)	19 (5)	70 (7)	21 (6)	9 (5)	…	…	2.2	1.5	…
Macigno sandstones – Tuscany (Cornamusini, 2002)											
Macigno Costiero petrofacies	57 (4)	19 (4)	24 (7)	66 (5)	19 (8)	15 (8)	≥13 ≥ 13	19	3	0.79	0.3
Macigno Intermedio petrofacies	55 (4)	27 (2)	18 (5)	75 (7)	19 (7)	6 (5)	≥13 ≥ 13	19	2.03	1.5	0.4
Macigno Appenninico petrofacies	59 (6)	25 (4)	16 (4)	82 (8)	11 (5)	7 (5)	<13	11.5	2.36	1.56	0.45
Macigno sandstones – Northern Umbria (Plesi et al., 2002)											
Poggio Belvedere member	40–55	20–50	10 –25	…	…	…	…	…	0.8–2.75	0.8–5	0.62
Macigno sandstones – NW Tuscany (Bruni et al., 2007)											
Upper Macigno	50 (6)	34 (8)	16 (4)	74 (9)	15 (7)	11 (8)	…	…	1.47	2.125	…
Lower Macigno	52 (3)	32 (4)	16 (2)	79 (8)	13 (6)	8 (5)	…	…	1.625	2	…
Macigno sandstones – E Tuscany/W Umbria (Barsella et al., 2009)											
Molin Nuovo member	49–74	28–42	9–26	42–59	30–38	6–20			1.2–2.6	1–4.7	…
Poggio Belvedere member	36–61	14–24	10–25	52–89	6–33	4–15	…	…	1.5–4.3	0.96–1.4	…
Modern Calabria Arc sands											
Granite sourced sands*	46	33	21	…	…	…	…	…	1.3	3.3	…
Metamorphic sourced sands*	55	24	21	…	…	…	…	…	2.4	1.4	…
Average*	51	28	21	88	0	12	0	0	1.82	1.33	…
Neto-Lipuda petrofacies**	36	46	18	86	0	14	0	0	0.78	2.55	0.7

Note: *Data reported after Ibbeken and Schleyer, 1991; ** Data reported after Perri et al., 2012b.

value $Rg_{65}Rv_3Rm_{32}$; $Rg_{62}Rs_9Rm_{29}$). Coarse gneissic fragments are rare. Micas grains, including either muscovite, biotite and chlorite, are abundant. Carbonate constituents are only present in R1, R2, and R9 samples, collected within calciturbidite levels, and R10 sample (Fig. 7H). Biofacies related to these levels are reported in detail in 5.1.

The interstitial component of siliciclastic arenites includes detrital fine siliciclastic matrix, and rare authigenic minerals and pseudomatrix. Only in the carbonate samples the interparticle porosity is partially filled by sparite and microsparite calcite cement and relatively fine carbonate matrix.

Differently to previous data of the Macigno Fm., the Renali sandstones are quite similar to those of the "Macigno Appenninico" of Northern Tuscany (Di Giulio, 1999: $Qm_{59}F_{29}Lt_{17}$; Bruni et al., 2007: average value, $Qm_{50}F_{34}Lt_{16}$) and the Poggio Belvedere Mb. sandstones of Trasimeno Lake area (Plesi et al., 2002; $Qm_{40\text{-}55}F_{20\text{-}}$

$_{50}Lt_{10-25}$; Barsella et al., 2009; $Qm_{36-61}F_{14-24}Lt_{10-25}$; Table 3). The lithic composition is quite similar to that reported by Cornamusini (2002) for the Macigno Costiero in Southern Tuscany ($Lm_{66}Lv_{19}Ls_{15}$). The volcanic lithic percentage is similar (Renali area: Lv = 13; Macigno Costiero: Lv > 13) although the means of volcanic index (Iv = Lv/L%) is properly more compatible with Macigno Fm. of Chianti Hills area (Renali: Iv = 11.25; Macigno Costiero: Iv = 19; Macigno del Chianti: Iv = 11.5. Data from Cornamusini, 2002; see Table 3 and Fig. 8).

c) Maestà Stratigraphic Section

Sandstones of the Maestà section are included in the lobe-fringe facies (M1 and M3 samples), basin plain facies (M8 sample) and slurried divisions (M5 sample). Sandstones are quartzofeldspathic (average value: $Qm_{64}F_{30}Lt_6$). The average Qm/F ratio is 2.52, the highest value in the Poggio Belvedere Mb.

The overall lithic content is less abundant than the other sections and the metasedimentary lithic fragments are always more abundant than the sedimentary fragments (average value: $Lm_{82}Lv_0Ls_{18}$; Fig. 6). Quartz grains are the most abundant constituents in all the studied facies and their amount reaches a large amount in laminated sandstones of lobe-fringe facies (F7 facies), sampled in the mid-top part of the section (M3 sample: Qm = 79%; Qm/F = 4.77). Quartz grains show high sorting and occur as subrounded and subspherical monocrystalline grains. Feldspars (both plagioclase and K-feldspars) are abundant, and plagioclase versus total feldspars ratio is high as well in Renali section (P/F = 0.76). The few metasedimentary lithic grains include fine-grained micaschist, comprising also few chloriteschist fragments, and rare slate and phyllite. Siltstone fragments are rare or absent, whereas chert grains are present (e.g. M1 sample; F4 facies). Phaneritic fragments of plutonic rocks occur, and metamorphic fragments result to prevail in some laminate sandstones (average value $Rg_{43}Rs_{10}Rm_{47}$). Coarse gneissic fragments are rare.

Similarly to Renali area, the Maestà sandstones can be compared to both Macigno Appenninico of Northern Tuscany (Di Giulio, 1999: $Qm_{59}F_{29}Lt_{17}$; Bruni et al., 2007: average value, $Qm_{50}F_{34}Lt_{16}$) and Poggio Belvedere sandstones of Trasimeno Lake (Barsella et al., 2009: $Qm_{36-61}F_{14-24}Lt_{10-25}$) (Fig. 7), although average feldspar is considerably higher, and lithic composition is subordinate. The lithic percentage is quite similar to that reported by Cornamusini (2002) for the Macigno del Chianti in Southern Tuscany ($Lm_{82}Lv_{11}Ls_7$), with differences in volcanic amount. These sandstones show some similar petrological characteristics with Renali sandstones excepting for average lithic component and missing of volcanic grains.

5.1. Biotic assemblage of calciturbidites

The samples collected in graded-laminated intervals of calciturbidites (R1 sample: F8 facies) (*rudstone* texture; Dunham, 1962; Embry and Klovan, 1971) comprise several mm to cm-sized ? Eocene to ?Early Miocene macroforaminifers, including mainly alveolinids, nummulitids and lepidocyclinids with small benthic shallow water and deep water foraminifers (Fig. 7H). Extrabasinal carbonate grains are present and they include biomicritic and peloidal limestones, coralline algae (*Rhodophyta*), thick shelled bivalves, echinoids and bryozoan fragments. Planktonic foraminifers (globigerinids) and porcelaneous small foraminifers (miliolids), coupled with radiolarians, sponge spicules and ostracods, have been recorded as mm-grained extrabasinal grains in wackestones. Samples from laminated-convolute facies (R9 and R2; F9a–b) have mixed carbonate-siliciclastic composition (hybrid arenites *sensu* Zuffa, 1980) with abundant skeletons of bivalves and benthic foraminifers, and angular silt-size quartz and micas grains.

5.2. Comparison with modern sand analogues

The studied detrital modes of the Macigno Fm. can be compared with the modern analogues continental and marine sands of Calabria reported from Ibbeken and Schleyer (1991), Critelli and Le Pera (1994, 1998, 2003), Le Pera et al. (2001), and Perri et al. (2012b) (Table 3). Valloni et al. (1991) and Di Giulio (1999) have done similar studies.

In general, the average value of the Macigno Fm. sandstones ($Qm_{57}F_{34}Lt_9$; this study) is quite similar to the average value of modern sands of Calabria ($Qm_{51}F_{28}Lt_{21}$, Ibbeken and Schleyer, 1991) except for a visible depletion in the fine-grained lithic component.

In detail, the mean of the detrital modes in sandstones of the Pianello Stratigraphic section ($Qm_{49}F_{40}Lt_{11}$, Qm/F = 1.33) are comparable with granite-sourced modern sands analyzed by Ibbeken and Schleyer (1991) in which the average value is $Qm_{46}F_{33}Lt_{21}$ with a Qm/F ratio of 1.3 (see Table 3). In particular W-oriented sandstones of the outer lobe-fringe facies ($Qm_{39}F_{46}Lt_{15}$, Qm/F = 0.94) are very similar with modern Calabrian sands of the Neto-Lipuda petrofacies ($Qm_{36}F_{46}Lt_{18}$, Qm/F = 0.8; data reported from Le Pera et al., 2001; Perri et al., 2012b) deposited in the Ionian sea offshore that is derived from a plutonic-dominated source area (Sila Massif).

Differently from Pianello stratigraphic section, detrital modes of the Renali (average value: $Qm_{58}F_{31}Lt_{11}$, Qm/F = 1.93) and the Maestà sandstones (average value: $Qm_{64}F_{30}Lt_6$, Qm/F = 2.52) show similar petrological characteristics with granitoid plus metamorphic-sourced modern Calabrian sands ($Qm_{55}F_{24}Lt_{21}$, Qm/F $\geq$ 2) reported from Ibbeken and Schleyer (1991). Thus, there is a visible depletion in felsic grains going from the Pianello toward the Renali and Maestà Stratigraphic sections (see Section 7).

6. Mineralogical and geochemical composition of mudstones

6.1. Mineralogy of mudstones

Whole-rock XRD analyses (Table 4) indicate that phyllosilicates are the main mineralogical components, ranging from 48% to 69% of the bulk rock. Illite and mica prevail with values up to 53%, whereas chlorite ranges from 10% to 25%. Kaolinite occurs in minor amounts. Among the interstratified minerals, the I–S mixed layers are slightly more abundant, but the amounts of C–S mixed layers are less abundant. The non-phyllosilicate minerals are represented by quartz, feldspars (plagioclase and K-feldspar) and carbonates (calcite and dolomite). Quartz ranges from 20% to 26%.The amount of K-feldspar ranges up to 2%, and the amount of plagioclase ranges from a few percent up to 19%. Dolomite is present in trace amounts in the PA1 and PA2 samples of the Pianello sections. Calcite occurs in all samples and it ranges from few percent up to 11% in the upper portion of the Pianello section and throughout the Renali section. Variation of mineral concentrations is related to the different source areas that influence the chemical and mineralogical composition of the sediments.

6.2. Whole-rock geochemistry of mudstones

Major- and trace-element concentrations are listed in Table 5. The studied mudstones have been plotted in the classification diagram for terrigenous rocks (Fig. 9). The SiO_2/Al_2O_3 ratio, the most commonly used parameter, reflects the relative abundance of quartz, feldspar and clay minerals (e.g., Potter, 1978). The studied samples plot in the field of shale, toward the wacke field, thus reflecting variation in the quartz–feldspars/mica ratio in the

Table 4
Mineralogical composition of the bulk rock (weight percent).

Section	Sample	Exp (I/S)	Exp (Chl/S)	Illite- micas	Kao	Chl	Σ Phy	Qtz	K-feld	Pl	Cal	Dol
Maestà area	MA4	1	1	32	tr	22	56	22	1	12	7	0
	MA1	1	1	29	tr	25	56	22	1	15	5	0
	MA3	3	2	37	1	19	62	26	1	9	2	0
Renali area	RA5	3	2	53	1	10	69	24	1	4	1	0
	RA4	2	2	32	tr	12	48	22	2	19	9	0
	RA3bis	1	1	32	tr	15	49	23	1	16	10	0
	RA3	2	1	32	tr	14	49	23	1	15	11	0
	RA1	1	1	35	tr	20	57	22	1	13	7	0
Pianello area	PA4	1	1	35	2	14	53	20	2	13	11	0
	PA3A	1	1	33	2	13	50	25	2	17	5	0
	PA2	2	1	48	1	13	65	24	2	7	2	tr
	PA1	1	2	34	tr	16	53	24	2	15	5	tr

studied samples.

Geochemical compositions of the studied mud samples and the Post-Archean Australian Shales (PAAS; Taylor and McLennan, 1985) were normalized to the to the Upper Continental Crust (UCC; McLennan et al., 2006) (Fig. 10).

The mudstones are characterized by narrow compositional ranges for SiO_2, Al_2O_3, MnO and K_2O, which have concentrations close to those of the UCC (Fig. 10). Sodium and phosphorous are strongly depleted relatively to UCC, but CaO is variable in concentration ranging from 1.65 (PA2) to 7.03 wt.% (PA4). The observed Na_2O depletion is likely due to the burial history of these samples, which promoted the formation of K-rich, mica-like clay minerals. The high CaO concentrations are related to the carbonate minerals present in some samples of Renali area, although the highest values of CaO have been also recorded within mudstones of Pianello area. Magnesium is enriched relatively to UCC, ranging from to 5.73 (PA2) to 9,69 wt.% (MA1), and its abundance is linked to occurrence of micas, as biotite and chlorite. Titanium and Fe_2O_3 values are also high. The general trend of the observed UCC pattern shows similar variations with those observed for the PAAS (Fig. 10).

Table 5
Major, trace element and ratios distribution of mudstone samples.

Sample	Pianello area				Renali area					Maestà area		
	PA1	PA2	PA3A	PA4	RA1	RA3	RA3bis	RA4	RA5	MA1	MA3	MA4
Oxides (wt%)												
SiO_2	53.29	53.17	53.05	48.04	50.56	49.66	49.76	50.64	52.57	49.44	54.30	49.65
TiO_2	0.80	0.89	0.82	0.80	0.82	0.78	0.81	0.79	0.99	0.86	0.85	0.84
Al_2O_3	15.81	17.82	15.54	14.82	15.55	14.26	14.74	14.65	18.61	15.37	17.12	15.28
Fe_2O_3	7.03	5.86	7.06	7.38	7.88	7.53	7.55	7.38	5.74	8.59	7.11	7.90
MnO	0.07	0.08	0.08	0.08	0.08	0.08	0.08	0.09	0.04	0.08	0.06	0.09
MgO	6.75	5.73	6.28	6.58	6.42	5.81	6.17	6.25	6.37	9.69	6.58	8.11
CaO	3.33	1.65	3.81	7.03	4.71	6.86	6.16	5.97	1.34	3.33	1.72	4.67
Na_2O	1.17	0.51	1.28	0.63	0.89	1.16	1.03	1.08	0.25	0.80	1.01	0.99
K_2O	3.59	4.43	3.39	3.54	3.44	2.99	3.22	3.20	5.11	2.95	4.08	3.10
P_2O_5	0.11	0.08	0.12	0.08	0.08	0.11	0.10	0.11	0.05	0.08	0.10	0.09
LOI	7.33	9.35	7.70	11.00	9.31	9.93	9.91	9.41	8.57	8.71	6.66	9.04
Tot	99.28	99.57	99.12	99.98	99.74	99.17	99.51	99.56	99.64	99.90	99.58	99.76
Trace elements (ppm)												
V	154.00	178.00	164.00	175.00	164.00	141.00	160.00	152.00	180.00	176.00	164.00	168.00
Cu	36.88	33.23	42.14	34.08	45.21	17.76	50.39	59.46	35.80	48.16	32.80	45.19
Co	20.62	22.70	21.22	29.99	31.88	20.82	22.97	18.61	20.56	32.31	17.62	34.51
Cr	132.00	237.00	158.00	196.00	247.00	107.00	173.00	177.00	243.00	592.00	188.00	393.00
Ni	90.47	137.89	101.60	164.48	168.86	85.79	133.06	136.12	152.40	363.56	108.28	266.88
Zn	119.52	111.38	117.22	134.23	145.62	113.41	137.94	139.97	101.54	129.40	131.52	130.47
Sr	141.00	103.00	150.00	249.00	190.00	228.00	247.00	224.00	96.00	129.00	101.00	185.00
Ba	479.00	346.00	471.00	417.00	463.00	439.00	434.00	435.00	300.00	393.00	444.00	438.00
Rb	193.00	254.00	179.00	197.00	187.00	146.00	170.00	164.00	304.00	156.00	221.00	159.00
Y	32.00	31.00	28.00	31.00	28.00	21.00	34.00	35.00	40.00	29.00	30.00	30.00
Zr	177.00	183.00	168.00	128.00	138.00	147.00	152.00	157.00	197.00	156.00	172.00	155.00
Nb	17.00	20.00	18.00	18.00	17.00	16.00	17.00	15.00	23.00	16.00	19.00	16.00
La	43.00	60.00	39.00	36.00	29.00	16.00	35.00	39.00	69.00	40.00	57.00	43.00
Ce	84.00	134.00	69.00	91.00	75.00	64.00	96.00	97.00	144.00	86.00	109.00	84.00
Ratios												
CIA	66.48	68.05	66.89	68.44	64.80	68.72	67.10	67.62	66.47	70.43	68.54	70.20
CIA'	68.54	69.95	68.65	69.79	70.08	69.35	69.47	69.21	69.04	72.80	68.68	71.03
ICV	1.43	1.07	1.46	1.75	1.55	1.76	1.69	1.68	1.06	1.71	1.25	1.68
La+Ce/Cr	0.96	0.82	0.68	0.65	0.42	0.75	0.76	0.77	0.88	0.21	0.88	0.32
La+Ce/Co	6.16	8.55	5.09	4.23	3.26	3.84	5.70	7.31	10.36	3.90	9.42	3.68
La+Ce/Ni	1.40	1.41	1.06	0.77	0.62	0.93	0.98	1.00	1.40	0.35	1.53	0.48
Al/K	4.40	4.02	4.59	4.19	4.52	4.77	4.58	4.58	3.64	5.21	4.19	4.93
Rb/K	0.005	0.006	0.005	0.006	0.005	0.005	0.005	0.005	0.006	0.005	0.005	0.005
Cr/V	0.86	1.33	0.96	1.12	1.51	0.76	1.08	1.16	1.35	3.36	1.15	2.34
Y/Ni	0.35	0.22	0.28	0.19	0.17	0.24	0.26	0.26	0.26	0.08	0.28	0.11

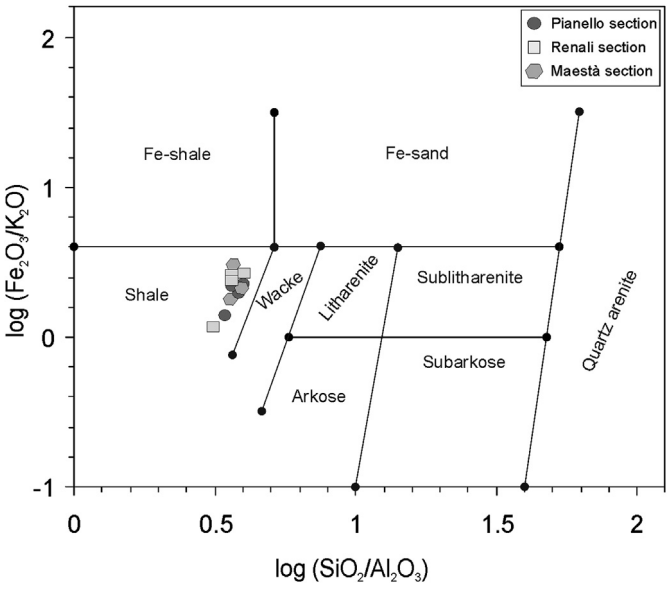

Fig. 9. Classification diagram for the studied mudstone samples (Herron, 1988).

In a ternary plot of SiO_2 (representing quartz), Al_2O_3 (representing mica/clay minerals), and CaO (representing carbonates), the mudstones of Poggio Belvedere Mb. can be described as mixtures of an aluminosilicate component with a small amount of carbonate phases (Fig. 11), although samples from Renali area and PA4 from Pianello area show higher Ca content than the average shales (PAAS).

These chemical associations and elemental variations are related to the mineralogical composition of the studied mudstones, as shown above by the mineralogical analyses.

7. Discussions

7.1. Provenance

Detrital signatures of the Poggio Belvedere Mb. of the Macigno Fm. contain an abundance of feldspars and coarse-grained phaneritic rock fragments, suggesting a source area of mostly plutonic and metamorphic rocks, with minor mafic magmatic and sedimentary rocks. Various ratios of feldspar, lithic fragment types, and quartz types in the sandstones reflect their transition between basement uplift and a transitional continental provenance type (Figs. 6–8; e.g. Dickinson, 1985). Sandstones of the Pianello Stratigraphic section of the Macigno Fm. are richer in F than those of the Renali and Maestà stratigraphic sections. The latter sections have a Q-enrichment trend.

Referring to other diagrams, studied sandstones plot at the RgRm side in either RgRvRm and RgRsRm diagrams (Critelli and Le Pera, 1994, 1995) and Lm in the LmLvLs diagram, confirming a transition between plutonic and metamorphic rock fragments. In detail, Pianello and Renali sandstones have an abundance of plutonic rock fragments, although some samples from the Renali area have a mixture of plutonic and metamorphic detritus. The Maestà sandstones plot between plutonic and metamorphic rock fragment field. This indicates a slight metamorphic trend. Petrological data indicate that sandstones of Pianello Stratigraphic section represent the results of prevalent drainage from an uplifted crystalline batholith with a dominance of granitoid rocks (granodiorite and tonalite) and minor metamorphic rocks (gneiss and schist) (Qm/F = 1.3; e.g. Ibbeken and Schleyer, 1991), whereas sandstones of the Renali and Maestà Stratigraphic sections reflect a provenance from a source area with a metamorphic-dominated basement (mica-schist, fine-grained schist and phyllite. Qm/F $\geq$ 2; e.g. Ibbeken and Schleyer, 1991). This suggests the occurrence of different pathways of drainage, resulting in a variation between a plutonic and metamorphic contribution and in quartz-feldspar ratio, or provenance from different but similar source areas, uplifted in the same time span. The main source area for the Macigno sandstones are inferred to be from the Western-Central Alps, located north and northwest from the Macigno foreland basin system.

The basement of the Western-Central Alps mainly consists of continental and oceanic-derived high pressure metamorphic rocks (blueschist and greenschist facies) including ophiolites, marbles, calce-schists, micas-schists, limestones, marls, and crystalline

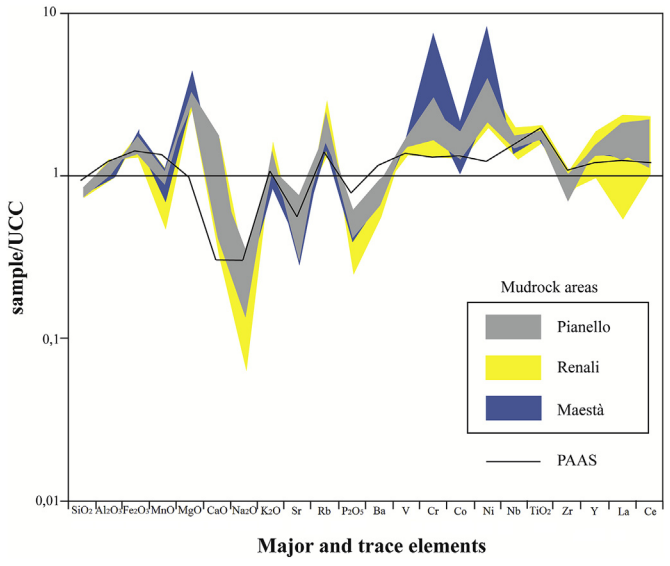

Fig. 10. Normalization of major and trace elements to the upper continental crust (UCC; McLennan et al., 2006). The plot of the Post-Archean Australian Shales (PAAS; Taylor and McLennan, 1985) is shown for comparison.

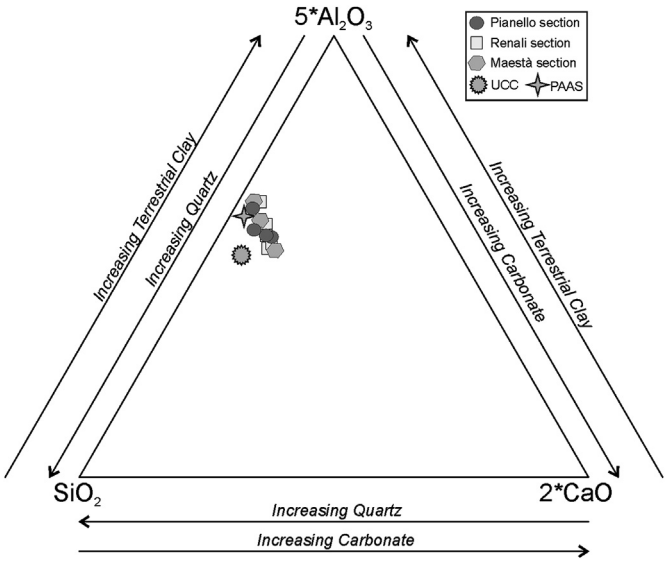

Fig. 11. Ternary plot showing the relative proportions of SiO_2 (representing quartz), Al_2O_3 (representing mica/clay minerals), and CaO (representing carbonate) for the studied mudstone samples.

rocks, derived from external massifs (i.e. Monte Rosa and Gran Paradiso Massifs and Dent Blanche complex). According to geological and geodynamic data, based on age and amount of uplift, surface extent of source area, and volume of uplifted rocks, the lithology of eroded rocks which were transferred to the Macigno foreland basin system can be inferred from the Ivrea–Verbano block (Di Giulio, 1999). Moreover the plutonic component of the Macigno Fm. sandstone could be related to less uplifted South Alpine crystalline basement of the Central Southern Alps (e.g. Bigi et al., 1990; Di Giulio, 1999). Its prevalent metamorphic composition, with only minor granite intrusions, is comparable with provenance constraints based on the Macigno sandstone detrital modes (average value $Qm_{54}F_{29}Lt_{17}$; Qm/F = 1.9) studied in previous works (e.g. Di Giulio, 1999). The compositional results closely correspond with detrital modes reported in overall sandstones of Poggio Belvedere Mb. of the present study (average value: $Qm_{57}F_{34}Lt_{9}$; Qm/F = 1.85), suggesting a general provenance from northwestward Alpine metamorphic-dominated domains. The occurrence of a volcanic signal, and sedimentary detritus, could be inferred from ophiolites and their sedimentary cover of Ligurian Nappe, although some volcanic grains, which have felsic granular texture with plagioclase phenocrysts, might also indicate a provenance from calc-alkaline trend volcanic arcs (i.e. Corsica–Sardinia block, Cornamusini et al., 2002).

The W-oriented granitic-sourced sandstones of the Pianello area testify to the influence of terrigenous material coming from a westernmost source area. The composition of these sandstones could correspond with source rocks of the Corsica–Sardinia block as Cornamusini et al. (2002) reported for the "Macigno Costiero" Fm. However, the minor content of volcanic lithic fragments, less abundant than in the "Macigno Costiero" Fm., and the location of Corsica–Sardinia during Late Oligocene–Early Miocene, which was relatively far from Umbria–Tuscany foreland basin system (Guerrera et al., 2015), also indicate the Alpine chain as W-derived crystalline source area (Fig. 12). The provenance of plutonic-dominated sandstones from the less uplifted Central Alps crystalline basement, located northwestward, do not explain the large amount of feldspars and phaneritic plutonic rock fragments (e.g. Pianello Stratigraphic section), which are clearly more abundant than other sandstones collected in the Macigno Apenninico (Valloni et al., 1991; Di Giulio, 1999; Dinelli et al., 1999; Cornamusini, 2002; Barsella et al., 2009). In detail, the distance between the Central Alpine crystalline basement and the Macigno basin of Trasimeno Lake area in the reconstructed palaeogeographic framework (Fig. 12) is estimated to be several hundred of kilometres. We suggest a provenance from Mesomediterranean terranes that were close to the basin. To support this conclusion, the Pianello lobe-fringe sandstones (F4 to F7 facies; Mutti, 1992), with the contribution of sudden decelerations of mud-rich turbidity currents (Type 1 Beds by Tinterri and Muzzi-Magahalaes, 2011), represent the final result of depositional processes starting from a plutonic-dominated source area that were very close to the Macigno foreland basin. The granite-sourced sandstones of Pianello area is inferred to have been derived by drainage of the Monte Rosa and Gran Paradiso massifs and Dent Blanche complex, located westward from the palaeo-Alps (Fig. 12), in which zircon fission-track ages of exhumation (related to almost 40 ma) are closely related with those of the Macigno sandstones (Dunkl et al., 2001).

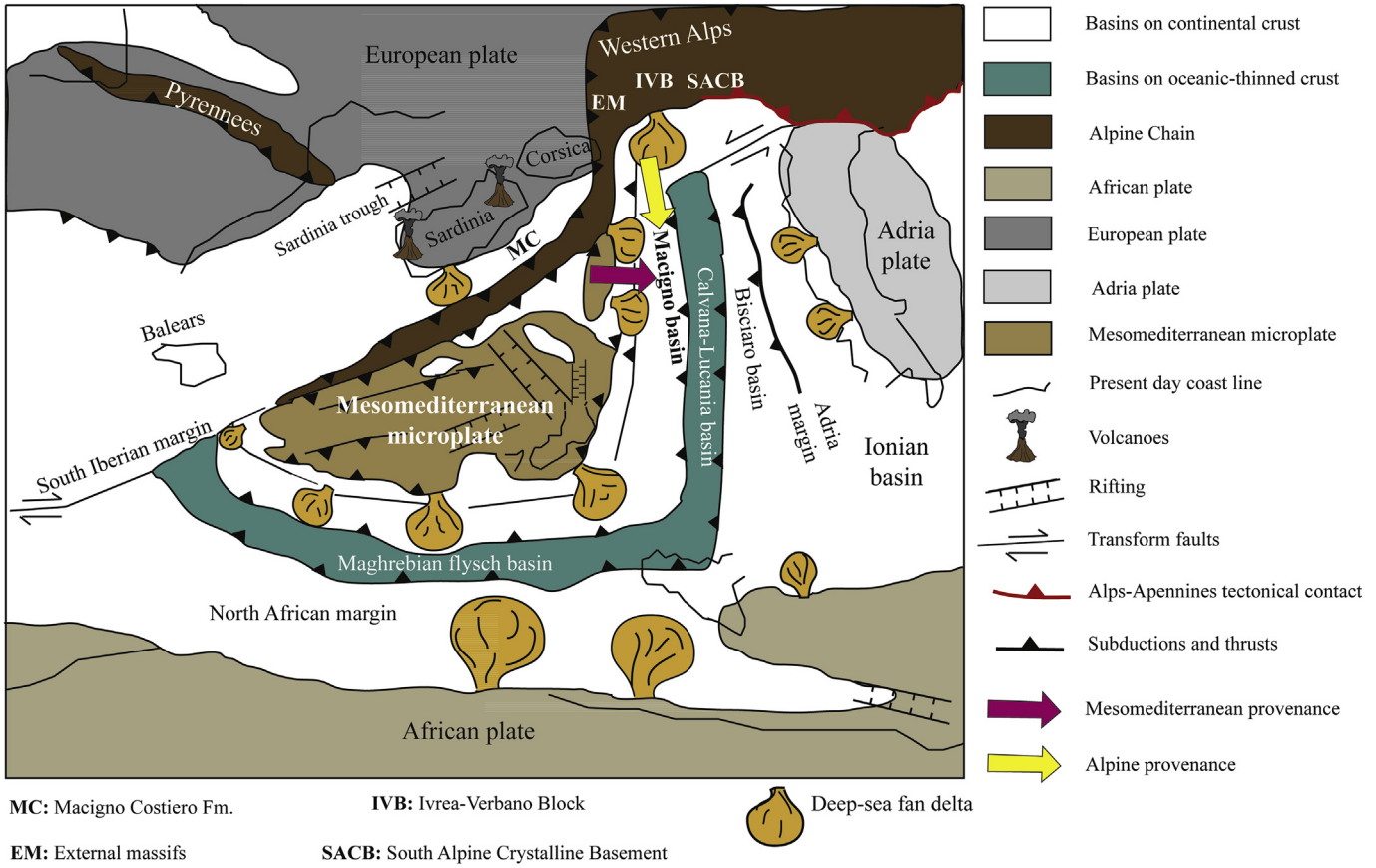

Fig. 12. Palaeogeographic and geodynamic model of the central-western Mediterranean area showing the possible source areas for Macigno foredeep system (modified after Guerrera et al., 2015).

The subordinate presence of extrabasinal carbonate detritus (e.g. Zuffa, 1985; Critelli et al., 2007) may suggests an additional source area composed of ?Eocene to early Miocene limestones, as shown by extrabasinal carbonate grains and fossils in the calciturbidites of the Renali area. The occurrence of benthic macroforams suggests a provenance from an external shelf environment, but wackestone-texture clasts including planktonic foraminifers (*globigerinids*) indicate a clear signal from an inner basin. Similar biofacies have been distinguished within calciturbidite and breccia levels of the Eocene-Oligocene Scaglia Toscana Fm. in the Chianti Hills area, in which traction features indicate palaeoflows towards the S and SW (Ielpi and Cornamusini, 2013) suggest a provenance from the Adria margin.

The variation among the LREEs (Light Rare Earth Elements; e.g., La and Ce) and the transition elements (e.g., Co, Cr and Ni) is considered a useful indicator in provenance studies (e.g., Culler, 2000; Perri et al., 2012b). The range of elemental ratios (La+Ce/Co, La+Ce/Cr, and La+Ce/Ni; Table 5) of all samples studied suggests a provenance from fairly felsic rather than mafic source-areas (e.g., Perri et al., 2012b). These ratio values do not exclude a supply of a mafic source, predominantly for the Maestà section that shows lower La+Ce/Cr (on average 0.47) and La+Ce/Ni (on average 0.79) than those of the Pianello and Renali sections (Table 5).

Generally, a low concentration of Cr and Ni indicates sediments derived from a felsic provenance, whereas, higher content of these elements are mainly found in sediments derived from ultramafic rocks (e.g., Wrafter and Graham, 1989; Armstrong-Altrin et al., 2004). Furthermore, the Cr/V ratio is an index of the enrichment of Cr over the other ferromagnesian trace elements, whereas Y/Ni monitors the general level of ferromagnesian trace elements (Ni) compared to a proxy for the HREE (Y). Mafic–ultramafic sources tend to have high ferromagnesian abundances; such a provenance would result in a decrease in Y/Ni ratios and an increase in Cr/V ratios (e.g., Hiscott, 1984; McLennan et al. 1993). The Cr/V *vs.* Y/Ni diagram (Hiscott, 1984) indicates a mixed source for the studied samples. In particular, the sediments are derived from a mainly felsic source area with a supply of a mafic source, predominantly for the Maestà section that shows Cr/V values ranging from 1.15 to 3.36 (Fig. 13). The V–Ni–La*10 diagram also suggests a similar provenance (e.g. Bracciali et al., 2007; Perri et al., 2011b) (Fig. 14), where the studied samples fall in an area related to provenance from a mixed source, mainly characterized by felsic rocks with a supply of mafic rocks. The mafic supply is probably related to the Ligurian ophiolites.

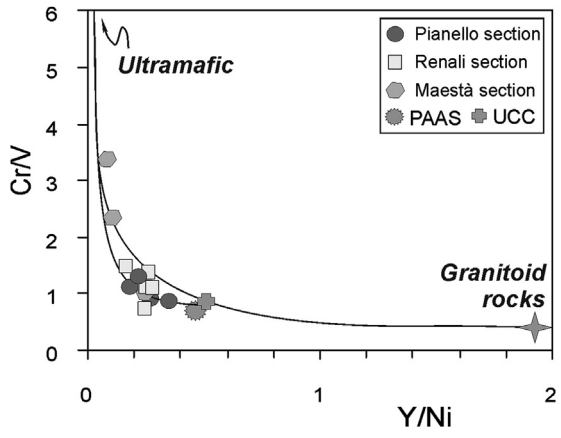

Fig. 13. Provenance diagram based on the Cr/V vs. Y/Ni relationships (after Hiscott, 1984). Curve model mixing between felsic and ultramafic end-members.

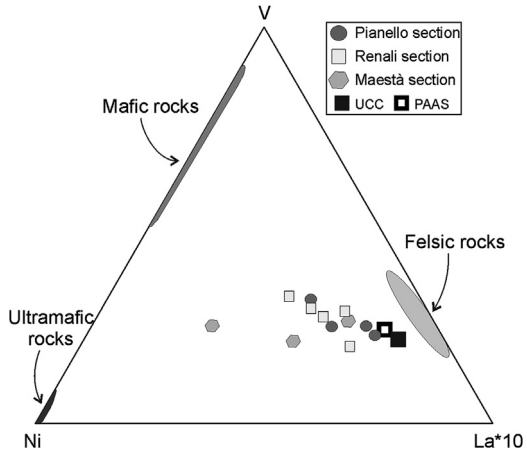

Fig. 14. V–Ni–La*10 ternary diagram, showing fields representative of felsic, mafic and ultramafic rocks plot separately (e.g., Bracciali et al., 2007; Perri et al., 2011b).

7.2. Source-area weathering

The evaluation of the source area weathering processes is mainly related to the variation of alkali and alkaline-earth elements in siliciclastic sediments. The Chemical Index of Alteration (CIA; Nesbitt and Young, 1982) is one of the most used indices to quantify the degree of source area weathering. Furthermore, when the sediments contain a high proportion of CaO, an alternative index of alteration CIA', expressed as molar volumes of [Al/(Al+Na+K)] × 100, has also used (e.g., Perri et al., 2014, 2015). The chemical compositions of studied mudstones are plotted as molar proportions within the A–CN–K and A–N–K diagrams. The CIA values of the studied samples are quite homogeneous (average = 66.4) with low-moderate values and in the A–CN–K triangular diagram the samples plot in a tight group on the A-K join close to the illite-muscovite point (Fig. 15A), suggesting low-moderate weathering conditions. Furthermore, the CIA' values of the mudrocks (average = 69.7) are quite similar to the CIA, typical of low-moderate weathering conditions. In the A–CN–K triangular diagram the samples plot in a tight group on the A-K join close to the illite-muscovite point (Fig. 15B). Micas (both illite and muscovite) are the dominant phyllosilicates occurring within the studied mudstones.

Simple ratios such as Al/K and Rb/K (e.g., Schneider et al., 1997; Roy et al., 2008), characterized by elements with contrasting mobility in the supracrustal environment, have been also used as a broad measure of weathering. Generally, high Al/K ratios are typical of sediments enriched in kaolinite, an important product of intensive weathering, over feldspar (or other K-bearing minerals). The Al/K ratios are low and constant (average = 4.47 ± 0.41) for all the studied sediments suggesting low-moderate weathering and no important fluctuations in weathering intensity, as also shown in the A–CN–K and A–N–K diagrams (Fig. 15). Furthermore, Rb/K ratios have been used to monitor source area weathering, where K is preferentially leached over Rb with increased intensity of weathering (Wronkiewicz and Condie, 1989, 1990; Peltola et al., 2008). Very low and homogeneous values of Rb/K ratios (<0.006) are found in the studied sediments, indicating weak to moderate weathering in a warm-humid climate (typical of the Mediterranean area) with minimal or negligible variations over time (e.g., Mongelli et al., 2012 and references therein).

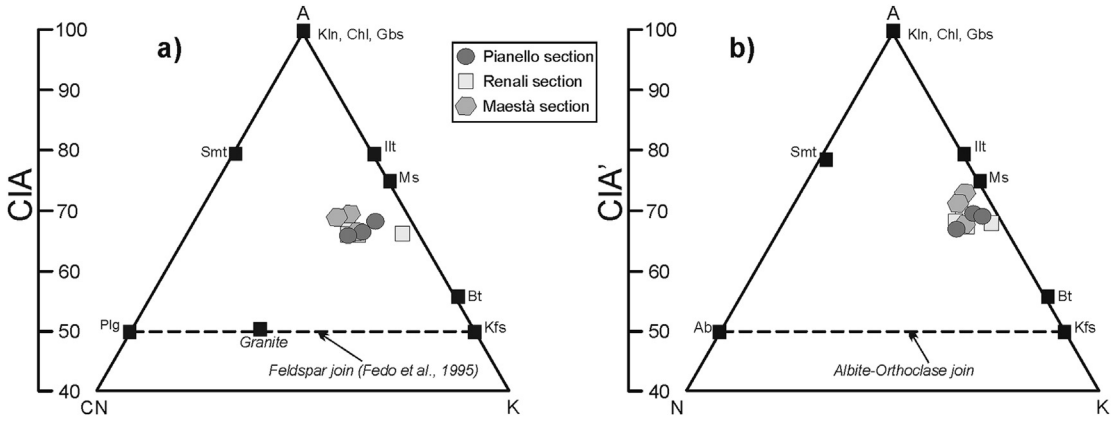

Fig. 15. Ternary (A) A–CN–K (Nesbitt and Young, 1982) and (B) A–C–N (Perri et al., 2014, 2015) plots. Key: A, Al_2O_3; C, CaO; N, Na_2O; K, K_2O; Gr, granite; Ms, muscovite; Ilt, illite; Kln, kaolinite; Chl, chlorite; Gbs, gibbsite; Smt, smectite; Plg, plagioclase; Kfs, K-feldspar; Bt, biotite; Ab, albite.

7.3. Sorting, transport and recycling

Generally, transport and deposition of terrigenous sediments involve mechanical sorting, that may affect the chemical composition of terrigeneous sediments and, thus, the distribution of source area weathering and provenance proxies (e.g., Mongelli et al., 2006; Perri et al., 2011a, 2012a, 2014).

Aluminum, titanium and zirconium are the major and minor elements generally considered the least mobile during chemical weathering (e.g. Perri et al., 2008a). Resistant minerals such as zircon, rutile and ilmenite generally host significant amounts of Ti and Zr. Variations in these elements are expressed in the Al–Ti–Zr ternary plot (García et al., 1994) that can highlight the possible effect of zircon addition mainly related to sorting and recycling processes. The studied mudstones plot in a tight area in the middle of the $15^*Al_2O_3$–Zr-300^*TiO_2 diagram (Fig. 16), and they are mostly characterized by homogeneuos values in the Al_2O_3/Zr ratio that could be due to poor recycling effects without a marked Zr enrichment (e.g., Perri et al., 2008a, 2011a; Caracciolo et al., 2011 and references therein).

The Index of Compositional Variability (Cox et al., 1995) has been generally used as a measure of compositional maturity. Immature mudstones, containing a high proportion of silicates other than clays, commonly show high values of this index (ICV>1), whereas mature mudstones, depleted in silicates other than clays, generally show low ICV values (ICV<1). Furthermore, immature mudrocks tend to be found in tectonically active settings and are characteristically first-cycle deposits (Van de Kamp and Leake, 1985), whereas mature mudrocks characterize tectonically quiescent or cratonic environments (Weaver, 1989) where sediment recycling is active. The studied sediments show ICV>1 (average = 1.51 ± 0.26) typical of first cycle, immature sediments where chemical weathering plays a minor role consistent with the medium-low CIA and CIA' values. Furthermore, the ICV values are also consistent with the sample distribution within the Al–Ti–Zr ternary plot that exclude recycling effects for the studied sediments, suggesting a very rapid transport in a depositional area close to the source(s). Such geochemical interpretation is totally compatible with ichnocoenosis, reported by Monaco and Trecci (2014). In fact the very large abundance of endichnial *Halopoa* (*H. embricata* and *H.* var. *fucusopsis*) suggests a basin floor environment rich in organic matter (i.e. phyto detritus) and diversified geochemical elements, extremely important to a proliferation of this ichnotaxon close to an alimentation source. Moreover the missing of *Avetoichnus luisae*, *Zoophycos* and *Nereites* trace fossils (see the ichnosubfacies at *Nereites*), occurring in the underlying Scaglia Toscana Fm. and in the overlying Marnoso Arenacea Fm., typical of distal deep-water areas, testifies to a very high sedimentation rate and the proximity of the depositional area to the source area. The differences among ichnotaxa is minimal in the three studied stratigraphic sections. However a slightly increasing on graphoglyptid abundance and diversification can be noted in the upper Renali and Maestà sections differently to the Pianello section (e.g. *Paleodictyon* and *Spirorhaphe*). This could be explained due to a progressive deepening of the basin plain environment.

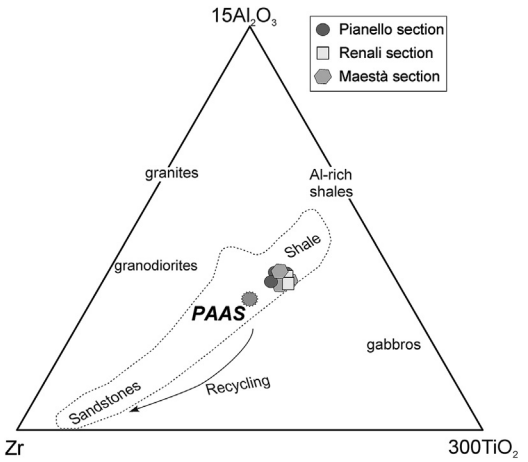

Fig. 16. Ternary $15^*Al_2O_3$–300^*TiO_2–Zr plot after García et al. (1994) for the studied mudstone samples.

The textural characteristics of the studied sandstones show moderate to low sorting, low degree of roundness of grains, and lack of altered quartz grains, confirming either poor recycling or closeness to the source area. However, sandstones at the Maestà Stratigraphic section are well sorted, indicating the settling of a fine-grained turbidite flow (F9 facies) in farthermost portion of the foredeep basin. Furthermore, the good sphericity of some clasts, their general equant-prolate shape, and their poor degree of flattering in outer lobe facies (F5–F7 facies in Pianello and Renali Stratigraphic sections) suggest that grains were initially reworked in a deltaic/fluvial sedimentary system and then resedimented into a deep-sea basin (e.g. Sames, 1966; Walker, 1975). Finally in Pianello Stratigraphic section the occurrence of well preserved continental vegetal remains and several slurried divisions indicate fast and sudden transport (e.g. hyperpicnal plumes), from a close source-

area which were more probably located westward, as well indicated by W-oriented sandy debris flows.

8. Conclusions

The Macigno Fm. sandstones, sampled in Poggio Belvedere Mb. in the Trasimeno Lake area, show a general quartzofeldspathic composition, but with some differences in the quartz/feldspar ratio (Qm/F) and in the composition of either phaneritic rock fragments and fine-grained lithic fraction.

The abundance of feldspars (lower Qm/F) and phaneritic plutonic and discrete occurrence of high-grade metamorphic rock fragments in lobe-fringe facies sandstones (F5–F7 facies) of the Pianello Stratigraphic section match those found in some granitoid-source modern sands of Calabria (Ibbeken and Schleyer, 1991; Perri et al., 2012b). These data, coupled with evidence of W-oriented flows, suggest a provenance from a granitoid-dominated batholith, and indicate the external massifs of the Western Alps (Monte Rosa and Gran Paradiso massifs, Dent Blanche complex) as a potential plutonic and high-grade metamorphic source area.

The overall NW–SE oriented fine-grained turbidites of the basin plain facies (F8 and F9a-b facies) and lobe-fringe sandstones of the Maestà Stratigraphic section have a higher Qm/F ratio than those of Pianello Stratigraphic section. They are characterized by a lower plutonic content, metamorphic lithic fragments, a fine-grained, low-medium grade metamorphic component, and subordinate volcanic lithic fragments in a similar amount with those studied previously in the sandstones of the Macigno Fm. (Di Giulio et al., 1999 and Barsella et al., 2009) and in metamorphic-source modern sands of Calabria (Ibbeken and Schleyer, 1991). These data mainly suggest a provenance from a metamorphic basement and a crystalline batholith that can be respectively identified with the Ivrea–Verbano block in Central-Western Alps and South Alpine crystalline basement in the Central Southern Alps (Di Giulio, 1999).

Volcanic and metavolcanic grains, coupled with Cr and Ni enrichment, mainly indicate a provenance from an ophiolitic unit and overlying sedimentary cover of the Ligurian Nappe. An enrichment of Nb and a peculiar occurrence of volcanic fragments with felsic granular fabric including plagioclase and quartz phenocrysts could be related to calco-alkaline rhyolites which characterize the Late Oligo-Early Miocene volcanic arc that originated by subduction of the Adria microplate beneath the eastern margin of Mesomediterranean continent (Guerrera et al., 2015). Finally the presence of East-derived calciturbidites in the Renali area including a typical biofacies of external shallow-water platform.

This detailed petrology coupled with sedimentological data (Monaco and Trecci, 2014) allows a better understanding of the spatial compositional evolution of the Macigno Fm., in agreement with the model for migrating foredeep basins proposed by Ricci Lucchi (1986). Firstly sedimentation developed in the western-most internal zones, which were transversally fed mainly by the crystalline basement of external massifs. During the migration of the orogenetic front and foredeep basin, the transversal feeders were substituted by longitudinal basin feeders from Western-Central Alps that were supplied with material similar to those from external massifs but with minor plutonic and high-grade metamorphic fragments. In the Late Oligocene–Early Miocene time interval, the Trasimeno Lake area was probably located in the distal external zones of Macigno foredeep that received terrigenous material firstly from the W–SW-oriented external massifs feeders (Pianello and lower Renali areas) and successively from the NW-oriented Central Alpine and S-oriented Apennine feeders (upper Renali and Maestà areas). Also ichnocoenoses seem to confirm this evolutionary trend. A similar compositional trend could be accounted for the Macigno Fm. in Northwestern Tuscany (Abetone area) analyzed by Bruni et al. (2007).

The geochemistry and mineralogy of Late Oligocene–Early Miocene deep-sea mudstones from Poggio Belvedere stratigraphic section of the Macigno Fm. suggest interesting palaeoclimatic and paleoweathering indications. The mudrocks have concentrations very similar to those of the UCC (McLennan et al., 2006) for Si, Al, Fe, Zr, K, whereas, Ca, Na, P, Ba and Sr are strongly depleted. Cesium and rubidium are slight enriched to the UCC and show a positive correlation with potassium, suggesting these trace elements are mostly hosted by dioctahedral mica-like clay minerals. This in turn indicates that illite and illitic minerals (I/S mixed layers) have played an important role in the distribution of elements in these rocks since these minerals are abundant in the studied samples. Furthermore, the mudstones fall in a tight group on the A–K join, in the A–CN–K triangular diagram, close to the muscovite point, in agreement with the mineralogical data. The Cr, Ni and Nb concentrations are enriched to the UCC, and indicate a trace of a mafic source.

The source area for the studied mudstones should have similar features to those of Western-Central Alps and crystalline external massifs basement, which are predominantly composed of felsic rocks with non-trivial amounts of mafic rocks. Geochemical proxies consistently suggest a felsic nature of the source area, with a minor but not negligible supply from mafic rocks that increased in the younger deposits (Maestà Stratigraphic section).

Both the CIA and the CIA' proxies suggest low-moderate weathering at the source area. The studied sediments seems to be affected by brief reworking in fluvial/deltaic zone and poor recycling processes and, as a consequence, it is likely these proxies monitor cumulative effects of weathering (e.g., Mongelli et al., 2006; Critelli et al., 2008; Perri et al., 2008a, 2008b).

The chemical weathering of such rocks under a humid climate season would produce an initial illitization of silicate minerals. Moreover, palaeocurrent analysis clearly indicates that terrigenous rocks derived from rapid erosion of highlands located to the N, NW, W and E of the present-day outcrops of the Trasimeno Lake area.

Acknowledgements

U. Amendola was supported by the “;CARICAL Fundation”; in Cosenza, Italy. Work supported by the MIUR-UNICAL Project (Relationships between Tectonic Accretion, Volcanism and Clastic Sedimentation within the Circum-Mediterranean Orogenic Belts, 2006–2011; Resp. S. Critelli). We are grateful to reviewers Manuel Martín-Martín, an anonymous reviewer and the Associate Editor Massimo Zecchin for reviews, helpful discussions, and comments on an earlier version of the manuscript.

References

Andreozzi, M., Di Giulio, A., 1994. Stratigraphy and petrography of the *M. Cervarola* sandstones in the type area, Modena Province. Mem. Soc. Geol. It. 48, 351–360.

Armstrong-Altrin, J.S., Lee, Y.I., Verma, S.P., Ramasamy, S., 2004. Geochemistry of sandstones from the upper miocene kudankulam Fm., southern India: implications for provenance, weathering, and tectonic setting. J. Sed. Res. 74, 285–297. http://dx.doi.org/10.1306/082803740285.

Aruta, G., 1994. Stratigraphy of the falterona and cervarola sandstones in the cortona area (Arezzo, northern Apennines). Mem. Soc. Geol. It. 48, 361–369.

Aruta, G., Pandeli, E., 1995. Lithostratigraphy of the m. Cervarola – m. Falterona Fm. between Arezzo and trasimeno Lake (Tuscan-Umbria, northern apennines, Italy). Giorn. Geol. 57 (1–2), 131–157 serie 3a.

Aruta, G., Bruni, P., Cipriani, N., Pandeli, E., 1998. The siliciclastic turbidite sequences of the tuscan domain in the val di Chiana-Val Tiberina area (eastern Tuscany and north-western Umbria). Mem. Soc. Geol. It. 52, 579–593.

Barsella, M., Boscherini, A., Botti, F., Marroni, M., Meneghini, F., Motti, A., Palandri, S., Pandolfi, L., 2009. Oligocene-Miocene foredeep deposits in the Lake Trasimeno area (Central Italy): insights into the evolution of the northern Apennines. Ital. J. Geosci. Boll. Soc. Geol. It.) vol. 128 (No. 2), 341–352. http://dx.doi.org/10.3301/

IJG.2009.128.2.341.
Basu, A., 1985. Reading provenance from detrital quartz. In: Zuffa, G.G. (Ed.), Provenance of Arenites. D. Reidel Publishing, Boston, pp. 231–247.
Bauluz, B., Mayayo, M.J., Fernandez-Nieto, C., Gonzalez Lopez, J.M., 2000. Geochemistry of precambrian and paleozoic siliciclastic rocks from the Iberian range (NE Spain): implications for source-area weathering, sorting, provenance, and tectonic setting. Chem. Geol. 168, 135–150. http://dx.doi.org/10.1016/S0009-2541(00)00192-3.
Bigi, G., Castellarin, A., Coli, M., Dal Piaz, G.V., Sartori, R., Scandone, P., Vai, G.B., 1990. Structural Model of Italy, Scale 1:500,000, Sheet N. 1. S.E.L.C.A. press, Florence.
Boccaletti, M., Calamita, F., Deiana, R., Gelati, R., Massari, F., Moratti, G., Ricci Lucchi, F., 1990. Migrating foredeep-thrust belt system in the northern Apennines and southern Alps. Palaeogeogr. Palaeoclimatol. Palaeoecol. 77, 3–14. http://dx.doi.org/10.1016/S0009-2541(00)00192-3.
Bracciali, L., Marroni, M., Luca, P., Sergio, R., 2007. Geochemistry and petrography of western tethys cretaceous sedimentary covers (Corsica and Northern Apennines): from source areas to configuration of margins. GSA Spec. Pap. 420, 73–93. http://dx.doi.org/10.1130/2006.2420(06).
Brozzetti, F., 2007. The Umbria Preapennines in the Monte Santa Maria Tiberina area: a new geological map with stratigraphic and structural notes. Boll. Soc. Geol. It. 126 (3), 511–529.
Bruni, P., Pandeli, E., 1980. Torbiditi calcaree nel Macigno e nelle Arenarie del Cervarola nell'area del Pratomagno e del Falterona (Appennino settentrionale). Mem. Soc. Geol. It. 21, 217–230.
Bruni, P., Pandeli, E., Nebbiai, M., 2007. Petrographic analysis in regional geology interpretation: case history of the Macigno (northern Apennines). In: Arribas, J., Critelli, S., Johnsson, M. (Eds.), Sedimentary Provenance: Petrographic and Geochemical Perspectives, Geological Society of America Special Paper 420, pp. 95–105. http://dx.doi.org/10.1130/2006.2420(07).
Canuti, P., Focardi, P., Sestini, G., 1965. Stratigrafia, correlazione e genesi degli Scisti Policromi dei monti del Chianti (Toscana). Boll. Soc. Geol. It. 84, 93–166.
Caracciolo, L., Le Pera, E., Muto, F., Perri, F., 2011. Sandstone petrology and mudstone geochemistry of the Peruc–Korycany Fm. (Bohemian cretaceous Basin, Czech Republic). Int. Geo. Rev. 53, 1003–1031. http://dx.doi.org/10.1080/00206810903429011.
Castellarin, A., 1992. Introduzione alla progettazione del profilo CROP. Studi Geol. Camerti, Spec. 1992 (2), 9–15.
Cavalcante, F., Fiore, S., Lettino, A., Piccarret, G., Tateo, F., 2007. Illite–smective mixed layers in silicide shales and piggy-back deposits of the Gorgoglione Fm. (Southern Apennines): geological inferences geodynamic implications. Bol. Soc. Geol. It 126, 241–254.
Centamore, E., Fumanti, F., Nisio, S., 2002. The Central northern apennines geological evolution from Triassic to Neogene time. Boll. Soc. Geol. It., Spec. 1, 181–197.
Condie, K.C., Noll, P.D.J., Conway, C.M., 1992. Geochemical and detrital mode evidence for-twosourcesofearlyProterozoicsedimentaryrocksfromtheTontoBasinSupergroup, central Arizona. Sed. Geol. 77, 51–76. http://dx.doi.org/10.1016/0037-0738(92)90103-X.
Condie, K.C., Lee, D., Farmer, G.L., 2001. Tectonic setting and provenance of the Neoproterozoic uinta mountain and Big Cottonwood groups, northern Utah: constraints from geochemistry, Nd isotopes, and detrital modes. Sed. Geol. 141, 443–464. http://dx.doi.org/10.1016/S0037-0738(01)00086-0.
Cornamusini, G., 2002. Compositional evolution of the Macigno Fm. of southern Tuscany along a transect from the Tuscan coast to the Chianti Hills. Boll. Soc. Geol. It. 1, 365–374.
Cornamusini, G., Elter, F.M., Sandrelli, F., 2002. The Corsica–Sardinia Massif as source area for the early northern Apennines foredeep system: evidence from debris flows in the "Macigno costiero" (Late Oligocene, Italy). Int. J. Earth Sci. Geol. Rundsch) 91, 280–290. http://dx.doi.org/10.1007/s005310100212.
Cox, R., Lowe, D., Cullers, R.L., 1995. The influence of sediment recycling and basement composition on evolution of mudrock chemistry in southwestern United States. Geochim. Cosmochim. Acta 59, 2919–2940. http://dx.doi.org/10.1016/0016-7037(95)00185-9.
Critelli, S., 1993. Sandstone detrital modes in the Paleogene Liguride Complex, accretionary wedge of the Southern Apennines (Italy). J. Sed. Res. 63, 464–476. http://dx.doi.org/10.1306/D4267B27-2B26-11D7-8648000102C1865D.
Critelli, S., 1999. The interplay of lithospheric flexure and thrust accomodation in forming stratigraphic sequences in the southern Apennines foreland basin system, Italy. Accad. Naz. dei Lincei Rendiconti Lincei Sci. Fis. Nat. 10, 257–326.
Critelli, S., Ingersoll, R.V., 1995. Interpretation of neovolcanic versus palaeovolcanic sand grains: an example from Miocene deep-marine sandstone of the Topanga group (southern California). Sedimentology 42, 783–804. http://dx.doi.org/10.1111/j.1365-3091.1995.tb00409.x.
Critelli, S., Le Pera, E., 1994. Detrital modes and provenance of Miocene sandstones and modern sands of the southern Apennines thrust-top basins (Italy). J. Sed. Res. 64, 824–835.
Critelli, S., Le Pera, E., 1995. Tectonic evolution of the southern Apennines thrust-belt (Italy) as reflected in modal compositions of Cenozoic sandstone. J. Geol. 103, 95–105.
Critelli, S., Le Pera, E., 1998. Post-Oligocene sediment dispersal systems and unroofing history of the Calabrian Microplate, Italy. Int. Geol. Rev. 48, 609–637.
Critelli, S., Le Pera, E., 2003. Provenance relations and modern sand petrofacies in an uplifted thrust-belt, northern Calabria, Italy. In: quantitative provenance studies in Italy. In: Valloni, R., Basu, A. (Eds.), Servizio Geologico Nazionale, Memorie Descrittive Della Carta Geologica D'Italia, 61, pp. 25–39.
Critelli, S., De Rosa, R., Platt, J.P., 1990. Sandstone detrital modes in the Makran accretionary wedge, southwest Pakistan: implications for tectonic setting and long-distance turbidite transportation. Sed. Geol. 68, 241–260. http://dx.doi.org/10.1016/0037-0738(90)90013-J.
Critelli, S., Le Pera, E., Galluzzo, F., Milli, S., Moscatelli, M., Perrotta, S., Santantonio, M., 2007. Interpreting siliciclastic-carbonate detrital modes in Foreland Basin Systems: an example from Upper Miocene arenites of the Central Apennines, Italy. In: Arribas, J., Critelli, S., Johnsson, M. (Eds.), Sedimentary Provenance: Petrographic and Geochemical Perspectives, GSA Special Paper 420, pp. 107–133. http://dx.doi.org/10.1130/2006.2420(08).
Critelli, S., Mongelli, G., Perri, F., Martin-Algarra, A., Martin-Martin, M., Perrone, V., Dominici, R., Sonnino, M., Zaghloul, M.N., 2008. Compositional and geochemical signatures for the sedimentary evolution of the Middle Triassic–Lower Jurassic continental redbeds from western-central Mediterranean Alpine chains. J. Geol. 116, 375–386. http://dx.doi.org/10.1086/588833.
Cullers, R.L., 2000. The geochemistry of shales, siltstones and sandstones of Pennsylvanian–Permian age, Colorado, USA: implications for provenance and metamorphic studies. Lithos 51, 181–203.
Damiani, A.V., Faramondi, S., Nocchi-Lucarelli, M., Pannuzi, L., 1987. Biocronostratigrafia delle unità litologiche costituenti "l'insieme varicolore" affiorante tra la Val di Chiana ed il fiume Tevere (Italia centrale). Boll. Serv. Geol. d'It. Roma 106, 109–160.
Di Giulio, A., 1999. Mass transfer from the Alps to the Apennines: volumetric constraints in the provenance study of the Macigno–Modino source–basin system, Chattian–Aquitanian, northwestern Italy. Sed. Geol. 124, 69–80. http://dx.doi.org/10.1016/S0037-0738(98)00121-3.
Dickinson, W.R., 1970. Interpreting detrital modes of greywacke and arkose. J. Sed. Petr. 40, 695–707.
Dickinson, W.R., 1985. Interpreting provenance relations from detrital modes of sandstones. In: Zuffa, G.G. (Ed.), Provenance of Arenites, North Atlantic Treaty Organization Advanced Study Institute Series, 148. D. Reidel, Dordrecht, The Netherlands, pp. 331–361. http://dx.doi.org/10.1007/978-94-017-2809-6.
Dinelli, E., Lucchini, F., Mordenti, A., Paganelli, L., 1999. Geochemistry of Oligocene–Miocene sandstones of the northern Apennines (Italy) and evolution of chemical features in relation to provenance changes. Sed. Geol. 127, 193–207. http://dx.doi.org/10.1016/S0037-0738(99)00049-4.
Dunham, R.J., 1962. Classification of carbonate rocks according to depositional texture. In: Ham, W.E. (Ed.), Classification of Carbonate Rocks, AAPG Memoir. 1, pp. 108–121.
Dunkl, I., Di Giulio, A., Kuhlemann, J., 2001. Combination of single-grain fission-track chronology and morphological analysis of detrital zircon crystals in provenance studies-sources of the Macigno Fm. (Apennines, Italy). J. Sed. Res. 71 (4), 516–525. http://dx.doi.org/10.1306/102900710516.
Einsele, G., 1991. Submarine mass flow deposits and turbidites. In: Einsele, G., Ricken, W., Seilacher, A. (Eds.), Cycles and Events in Stratigraphy. Springer, Berlin, pp. 313–339.
Embry III, A.F., Klovan, J.S., 1971. A late devonian reef tract on northeastern Banks Island, N.W.T. Bull. Can. Petrol. Geol. 4, 730–781.
Flanagan, F.J., 1976. Descriptions and Analyses of Eight New USGS Rock Standards, p. 192. U.S. Geological Survey Professional Paper 840, Washington.
Folk, R.L., 1968. Petrology of Sedimentary Rocks. University of Texas Publication, Austin, p. 170.
Gandolfi, G., Paganelli, L., Zuffa, G.G., 1983. Petrology and dispersal pattern in the Marnoso-arenacea Fm. (Miocene, Northerh Apennines). J. Sed. Petr 53, 493–507. http://dx.doi.org/10.1306/212F8215-2B24-11D7-8648000102C1865D.
García, D., Fonteilles, M., Moutte, J., 1994. Sedimentary fractionations between Al, Ti, and Zr and the genesis of strongly peraluminous granites. J. Geol. 102, 411–422.
Gazzi, P., 1966. Le arenarie del Flysch sopracretaceo dell'Appennino modenese; correlazioni con il Flysch di Monghidoro. Miner. Petrografica Acta 12, 69–97.
Graham, S.A., Ingersoll, R.V., Dickinson, W.R., 1976. Common provenance for lithic grains in carboniferous sandstones from ouachita mountains and black warrior basin. Jour. Sed. Petrol. 46, 620–632. http://dx.doi.org/10.1306/212F7009-2B24-11D7-8648000102C1865D.
Guerrera, F., Martín-Algarra, A., Martín-Martín, M., 2012a. Tectono-sedimentary evolution of the "Numidian Formation" and Lateral Facies (southern branch of the western Tethys): constraints for centralwestern Mediterranean geodynamics. Terra Nova 24, 34–41.
Guerrera, F., Tramontana, M., Donatelli, U., 2012b. Space/time tectono-sedimentary evolution of the umbria -Romagna-Marche miocene Basin (North apennines, Italy). Swiss J. Geosci. 105, 325–341.
Guerrera, F., Martin-Martin, M., 2014. Geodynamic events reconstructed in the Betic, Maghrebian, and Apennine chains (central-western Tethys). Bull. Soc. Géol Fr. 185, 329–341.
Guerrera, F., Martìn-Martìn, M., Raffaelli, G., Tramontana, M., 2015. The Early Miocene "Bisciaro volcaniclastic event" (northern Apennines, Italy): a key study for the geodynamic evolution of the central-western Mediterranean. Int. J. Earth Sci. Geol. Rundsch) 104, 1083–1106. http://dx.doi.org/10.1007/s00531-014-1131-5.
Herron, M.M., 1988. Geochemical classification of terrigenous sands and shales from core or log data. J. Sed. Petr. 58, 820–829. http://dx.doi.org/10.1306/212F8E77-2B24-11D7-8648000102C1865D.
Hill, K.C., Hayward, A.B., 1988. Structural constraints on the Tertiary plate tectonic evolution of Italy. Mar. Pet. Geol. 5, 2–16. http://dx.doi.org/10.1016/0264-8172(88)90036-0.

Hiscott, R.N., 1984. Ophiolitic source rocks for Taconic-age flysch: trace element evidence. Geol. Soc. Am. 95, 1261–1267. http://dx.doi.org/10.1130/0016-7606(1984)95<1261:OSRFTF>2.0.CO;2.
Ibbeken, H., Schleyer, R., 1991. Source and Sediment. A Case Study of Provenance and Mass Balance at an Active Plate Margin (Calabria, Southern Italy). Springer, Berlin.
Ielpi, A., Cornamusini, G., 2013. An outer ramp to basin plain transect: interacting pelagic and calciturbidite deposition in the Eocene–Oligocene of the Tuscan Domain, Adria Microplate (Italy). Sed. Geol. 294, 83–104. http://dx.doi.org/10.1016/j.sedgeo.2013.05.010.
Ingersoll, R.V., Suczek, C.A., 1979. Petrology and provenance of Neogene Sand from Nicobarand Bengalfans, DSDP sites 211and 218. J. Sed. Petr. 49, 1217–1228. http://dx.doi.org/10.1306/212F78F1-2B24-11D7-8648000102C1865D.
Ingersoll, R.V., Bullard, T.F., Ford, R.L., Grimm, J.P., Pickle, J.D., Sares, S.W., 1984. The effect of grain size on detrital modes: a test of the Gazzi–Dickinson point-counting method. J. Sed. Petr. 54, 103–116. http://dx.doi.org/10.1306/212F83B9-2B24-11D7-8648000102C1865D.
Johnsson, M.J., 1993. The system controlling the composition of clastic sediments. In: Johnsson, M.J., Basu, A. (Eds.), Processes Controlling the Composition of Clastic Sediments: GSA Special Paper, 284, pp. 1–19. http://dx.doi.org/10.1130/SPE284-p1.
Krumm, S., 1996. WINFIT 1.2: version of November 1996 (The Erlangen geological and mineralogical software collection) of "WINFIT 1.0: a public domain program for interactive profile-analysis under WINDOWS. In: XIII Conference on Clay Mineralogy and Petrology, Praha, 1994: Acta Universitatis Carolinae Geologica, 38, pp. 253–261.
Le Pera, E., Arribas, J., Critelli, S., Tortosa, A., 2001. The effects of source rocks and chemical weathering on the petrogenesis of siliciclastic sand from the Neto river (Calabria, Italy): implications for provenance studies. Sedimentology 48, 357–378.
McLennan, S.M., Hemming, D.K., Hanson, G.N., 1993. Geochimical aproaches to sedimentation, provenance and tectonics. Geol. Soc. Am. Spec. Pap. 284, 21–40.
McLennan, S.M., Taylor, S.R., Hemming, S.R., 2006. Composition, differentiation, and evolution of continental crust: constraints from sedimentary rocks and heat flow. In: Brown, M., Rushmer, T. (Eds.), Evolution and Differentiation of the Continental Crust. Cambridge University Press, Cambridge, pp. 92–134.
Milighetti, M., Monaco, P., Checconi, A., 2009. Caratteristiche sedimentologico-ichnologiche delle unità silicoclastiche oligo-mioceniche nel transetto Pratomagno-Verghereto, Appennino Settentrionale. Annali dell'Università degli Studi di Ferrara. Museol. Sci. Nat. 5, 23–129.
Monaco, P., Trecci, T., 2014. Ichnocoenoses in the macigno turbidite basin system, lower miocene, trasimeno (Umbrian apennines, Italy). Ital. J. Geo. 133, 116–130. http://dx.doi.org/10.3301/IJG.2013.18.
Monaco, P., Uchman, A., 1999. Deep-sea ichnoassemblages and ichnofabrics of the Eocene Scisti varicolori beds in the Trasimeno area, western Umbria, Italy. In: Farinacci, A., Lord, A.R. (Eds.), Depositional Episodes and Bioevents. Paleopelagos, Univ. La Sapienza, Spec. Publ., Roma, pp. 39–52.
Monaco, P., Milighetti, M., Checconi, A., 2009. Ichnocoenoses in the Oligocene to Miocene foredeep basins (Northern Apennines, central Italy) and their relation to turbidite deposition. Acta Geol. Pol. 60 (1), 53–70.
Monaco, P., Trecci, T., Uchman, A., 2012. Taphonomy and ichnofabric of the trace fossil Avetoichnus luisae Uchman & Rattazzi, 2011 in Paleogene deep-sea fine-grained turbidites: examples from Italy, Poland and Spain. Boll. Soc. Paleontol. Ital. 51 (1), 1–16.
Mongelli, G., Critelli, S., Perri, F., Sonnino, M., Perrone, V., 2006. Sedimentary recycling, provenance and paleoweathering from chemistry and mineralogy of Mesozoic continental redbed mudrocks, Peloritani Mountains, Southern Italy. Geochem. J. 40, 197–209.
Mongelli, G., Mameli, P., Oggiano, G., Sinisi, R., 2012. Messinian palaeoclimate and palaeo-environment in the western Mediterranean realm: insights from the geochemistry of continental deposits of NW Sardinia (Italy). Int. Geol. Rev. 54, 971–990. http://dx.doi.org/10.1080/00206814.2011.588823.
Mutti, E., 1992. In: AGIP, S.p.a. (Ed.), Turbitite Sandstones. S. Donato Milanese, p. 275.
Muzzi Magalhaes, P., Tinterri, R., 2010. Stratigraphy and depositional setting of slurry and contained (reflected) beds in the Marnoso-arenacea Fm. (Langhian Serravallian) Northern Apennines, Italy. Sedimentology 57, 1685–1720. http://dx.doi.org/10.1111/j.1365-3091.2010.01160.x.
Nesbitt, H.W., Young, G.M., 1982. Early Proterozoic climates and plate motions inferred from major element chemistry of lutites. Nature 299, 715–717. http://dx.doi.org/10.1038/299715a0.
Nesbitt, H.W., Young, G.M., McLennan, S.M., Keays, R.R., 1996. Effects of chemical weathering and sorting on the petrogenesis of siliciclastic sediments, with implications for provenance studies. J. Geol. 104, 525–542.
Peltola, P., Brun, C., Strom, M., Tomilia, O., 2008. High K/Rb ratios in stream waters. Exploring plant litter decay, ground water and lithology as potential controlling mechanisms. Chem. Geol. 257, 92–100. http://dx.doi.org/10.1016/j.chemgeo.2008.08.009.
Pandeli, E., Ferrini, G., Lazzari, D., 1994. Lithofacies and petrography of the Macigno Fm. from the Abetone to the Monti del Chianti areas (Northern Apennines). Mem. Soc. Geol. Ital. 48, 321–329.
Perri, F., 2008. Clay mineral assemblage of the Triassic–Jurassic mudrocks from Western-Central mediterranean regions. Per. Mineral. 77, 23–40. http://dx.doi.org/10.2451/2008PM0002.
Perri, F., 2014. Composition, provenance and source weathering of Mesozoic sandstones from Western-Central Mediterranean Alpine Chains. J. Afr. Earth Sci. 91, 32–43. http://dx.doi.org/10.1016/j.jafrearsci.2013.12.002.
Perri, F., Rizzo, G., Mongelli, G., Critelli, S., Perrone, V., 2008a. Zircon compositions of lower Mesozoic redbeds of the Tethyan margins, West-Central mediterranean area. Int. Geol. Rev. 50, 1022–1039. http://dx.doi.org/10.2747/0020-6814.50.11.1022.
Perri, F., Cirrincione, R., Critelli, S., Mazzoleni, P., Pappalardo, A., 2008b. Clay mineral assemblages and sandstone compositions of the Mesozoic Longobucco Group, northeastern Calabria: implications for burial history and diagenetic evolution. Int. Geol. Rev. 50, 1116–1131. http://dx.doi.org/10.2747/0020-6814.50.12.1116.
Perri, F., Critelli, S., Mongelli, G., Cullers, R.L., 2011a. Sedimentary evolution of the Mesozoic continental redbeds using geochemical and mineralogical tools: the case of upper triassic to lowermost Jurassic M.te di Gioiosa mudstones (Sicily, Southern Italy). Int. J. E. Sc. 100, 1569–1587. http://dx.doi.org/10.1007/s00531-010-0602-6.
Perri, F., Muto, F., Belviso, C., 2011b. Links between composition and provenance of Mesozoic siliciclastic sediments from western Calabria (southern Italy). Ital. J. Geosci. 130, 318–329. http://dx.doi.org/10.3301/IJG.2011.04.
Perri, F., Critelli, S., Cavalcante, F., Mongelli, G., Dominici, R., Sonnino, M., De Rosa, R., 2012a. Provenance signatures for the Miocene volcaniclastic succession of the Tufiti di Tusa Fm., southern Apennines. Italy. Geol. Mag. 149, 423–442. http://dx.doi.org/10.1017/S001675681100094X.
Perri, F., Critelli, S., Dominici, R., Muto, F., Tripodi, V., Ceramicola, S., 2012b. Provenance and accommodation pathways of late Quaternary sediments in the deep-water northern ionian basin, southern Italy. Sed. Geo. 280, 244–259. http://dx.doi.org/10.1016/j.sedgeo.2012.01.007.
Perri, F., Borrelli, L., Gullà, G., Critelli, S., 2014. Chemical and minero-petrographic features of Plio-Pleistocene fine-grained sediments in Calabria, southern Italy. Ital. J. Geosci. 133, 101–115. http://dx.doi.org/10.3301/IJG.2013.17.
Perri, F., Ohta, T., 2014. Paleoclimatic conditions and paleoweathering processes on Mesozoic continental redbeds from Western-Central Mediterranean Alpine Chains. Palaeogeogr. Palaeoclimatol. Palaeoecol. 395, 144–157. http://dx.doi.org/10.1016/j.palaeo.2013.12.029.
Perri, F., Dominici, R., Critelli, S., 2015. Stratigraphy, composition and provenance of argillaceous marls from the Calcare di Base Fm., Rossano Basin (northeastern Calabria). Geol. Mag. 152, 193–209. http://dx.doi.org/10.1017/S0016756814000089.
Perrone, V., Perrotta, S., Marsaglia, K., Di Staso, A., Tiberi, V., 2013. The Oligocene ophiolite-derived breccias and sandstones of the Val Marecchia Nappe: insights for paleogeography and evolution of Northern Apennines (Italy). Palaeogeo. Palaeoclim. Palaeoecol. 394, 128–143.
Piccioni, R., Monaco, P., 1999. Caratteri sedimentologici, ichnologici e micro-paleontologici delle unità eoceniche degli scisti varicolori nella sezione di M. Solare. Boll. Serv. Geol. D'it. 143–188. CXV.
Plesi, G., Luchetti, L., Boscherin, A., Botti, F., Brozzetti, F., Bucefalo Palliani, R., Daniele, G., Motti, A., Nocchi, M., Rettori, R., 2002. The Tuscan successions of the high Tiber Valley (Foglio 289-Città di Castello): biostratigraphic, petrographic and structural features, regional correlations. Boll. Soc. Geol. It. 121 (1), 425–436.
Potter, P.E., 1978. Petrology and chemistry of modern big river sands. J. Geol. 86, 423–449.
Ricci Lucchi, F., 1986. The Oligocene to recent foreland basins of the northern Apennines. Int. Assoc. Sedimentol. Spec. Publ. 8, 105–139.
Ricci Lucchi, F., 1990. Turbidites in foreland and on-thrust basins of the northern Apennines. Palaeogeogr. Palaeoclimatol. Palaeoecol. 77, 51–66. http://dx.doi.org/10.1016/0031-0182(90)90098-R.
Ricci Lucchi, F., Valmori, E., 1980. Basin-wide turbidites in a Miocene, oversupplied deep-sea plain: a geometrical analysis. Sedimentology 27, 241–270. http://dx.doi.org/10.1111/j.1365-3091.1980.tb01177.x.
Roy, P.D., Caballero, M., Lozano, R., Smytatz-Kloss, W., 2008. Geochemistry of late quaternary sediments from Tecomuco lake, central Mexico: implication to chemical weathering and provenance. Chem. Erde 68, 383–393. http://dx.doi.org/10.1016/j.chemer.2008.04.001.
Sames, C.W., 1966. Morphometric data of some recent pebble associations and their applications to ancient deposits. J. Sed. Petr 36, 126–142.
Schneider, R.R., Price, B., Muller, P.J., Kroon, D., Alexander, I., 1997. Monsoon-related variations in Zaire (Congo) sediment load and influence of fluvial silicate supply on marine productivity in the east equatorial Atlantic during the last 200,000 years. Paleoceanography 12, 463–481. http://dx.doi.org/10.1029/96PA03640.
Shanmugan, G., 2002. Ten turbidite myths. Earth Sci. Rev. 58, 311–341. http://dx.doi.org/10.1016/S0012-8252(02)00065-X.
Suttner, L.J., 1974. Sedimentary petrographic province: an evaluation. Soc. Econ. Paleontol. Miner. Spec. Publ. 21, 75–84.
Talling, P.J., Amy, L.A., Wynn, R.B., Peakall, J., Robinson, M., 2004. Beds comprising debrite sandwiched within co-genetic turbidite: origin and widespread occurrence in distal depositional environments. Sedimentology 51, 163–194. http://dx.doi.org/10.1111/j.1365-3091.2004.00617.x.
Taylor, S.R., McLennan, S.M., 1985. The Continental Crust: its Composition and Evolution. Blackwell, Oxford.
Tinterri, R., Muzzi Magalhaes, P., 2011. Synsedimentary structural control on foredeep turbidites: an example from Miocene Marnoso-arenacea Fm., Northern Apennines. Italy. Mar. Petrol. Geol. 28, 629–657. http://dx.doi.org/10.1016/j.marpetgeo.2010.07.007.
Trecci, T., Monaco, P., 2011. Le ichnocenosi delle successioni sedimentarie Eocenico-Mioceniche affioranti tra il Lago Trasimeno e l'Alpe di Poti (Appennino

Settentrionale). Annali di Ferrara. Museol. Sci. Nat. 7, 1–101.
Trincardi, F., Verdicchio, G., Asioli, A., 2005. Comparing Adriatic contourite deposits and other Mediterranean examples. In: F.I.S.T. (Ed.), GeoItalia 2005, Spoleto 21-23 Settembre 2005, p. 321.
Valloni, R., Lazzari, D., Calzolari, M.A., 1991. Selective alteration of arkose framework in Oligo-Miocene turbidites of the Northern Apeninnes foreland: impact on sedimentary provenance analysis. In: Morton, A.C., Todd, S.P., Haughtpn, P.D.W. (Eds.), 1991, Developments in Sedimentary Provenance Studies, GSA Special Publication, No 57, pp. 125–136. http://dx.doi.org/10.1144/GSL.SP.1991.057.01.11.
Van de Kamp, P.C., Leake, B.E., 1985. Petrography and geochemistry of feldspathic and mafic sediments of the northeastern Pacific margin. Trans. R. Soc. Edinb. Earth Sci. 76, 411–449.
Van der Meulen, M.J., Meulenkamp, J.E., Wortel, M.J.R., 1998. Lateral shifts of Apenninic foredeep depocentres reflecting detachment of subducted lithosphere. EPSL 154, 203–219. http://dx.doi.org/10.1016/S0012-821X(97)00166-0.
Walker, R.G., 1975. Generalized facies model for resedimented conglomerates of turbidite association. Bull. Geol. Soc. Am. 86, 737–748. http://dx.doi.org/10.1130/0016-7606(1975)86<737:GFMFRC>2.0.CO;2.
Weaver, C.E., 1989. Clays, Muds, and Shales. In: Developments in Sedimentology, 44. Elsevier, Amsterdam, ISBN 0-444-87381-3, p. 819.
Wrafter, J.P., Graham, J.R., 1989. Ophiolitic detritus in the Ordovician sediments of South Mayo Ireland. J. Geol. Soc. Lond. 146, 213–215. http://dx.doi.org/10.1144/gsjgs.146.2.0213.
Wronkiewicz, D.J., Condie, K.C., 1989. Geochemistry and provenance of sediments from the Pongola Supergroup, South Africa: evidence for a 3.0 Ga old continental craton. Geochem. Cosmochim. Acta 53, 1537–1549. http://dx.doi.org/10.1016/0016-7037(89)90236-6.
Wronkiewicz, D.J., Condie, K.C., 1990. Geochemistry and mineralogy of sediments from the ventersdorp and transvaal supergroup, South Africa: cratonic evolution during the early Proterozoic. Geochim. Cosmochim. Acta 54, 343–354. http://dx.doi.org/10.1016/0016-7037(89)90236-6.
Zaghloul, M.N., Critelli, S., Perri, F., Mongelli, G., Perrone, V., Sonnino, M., Tucker, M., Aiello, M., Ventimiglia, C., 2010. Depositional systems, composition and geochemistry of Triassic rifted continental margin redbeds of Internal Rif Chain, Morocco. Sedimentology 57, 312–350. http://dx.doi.org/10.1111/j.1365-3091.2009.01080.x.
Zuffa, G.G., 1980. Hybrid arenites: their composition and classification. J. Sed. Petrol. 50, 21–29. http://dx.doi.org/10.1306/212F7950-2B24-11D7-8648000102C1865D.
Zuffa, G.G., 1985. Optical analyses of arenites: influence of methodology on compositional results. In: Zuffa, G.G. (Ed.), Provenance of Arenites. Dordrecht, The Netherlands, NATO Advanced Study Institute Series, Reidel, 148, pp. 165–189. http://dx.doi.org/10.1007/978-94-017-2809-6_8.
Zuffa, G.G., 1987. Unravelling hinterland and offshore palaeo- geography from deep-water arenites. In: Leggett, J.K., Zuffa, G.G. (Eds.), Marine Clastic Sedimentology, Models and Case Studies. Graham and Trotman, London, pp. 39–61. http://dx.doi.org/10.1007/978-94-009-3241-8_2.